University Medical Center Göttingen

Georg-August-University

Master program Molecular Medicine

Wild-type p53 suppresses the tumor-driving HSF1 activity in colorectal cancer

Master's Thesis

submitted by

Özge Çiçek Şener

born in Ankara, Turkey

Institute of Molecular Oncology

Göttingen, May 2018

Data Sheet

Title of thesis	Wild-type p53 suppresses the tumor-driving HSF1 activity in colorectal cancer
Department	Molecular Oncology, University Medicine Göttingen Göttingen Center for Molecular Biosciences (GZMB) Ernst Caspari Haus Justus von Liebig Weg 11, 37077 Göttingen
Name, Given Name	Özge Çiçek Şener
Matriculation Number	21617418
Address	Hannoversche Strasse 152b, WE 117 Göttingen, 37077
Phone	+4915754740888
E-mail	ozgecicek.sener@stud.uni-goettingen.de
First reviewer	Prof. Dr. Matthias Dobbelstein
Contact details	mdobbel@uni-goettingen.de
Internal supervisor	Dr. Ramona Schulz-Heddergott
Second reviewer	
Contact details	
Handover date	28.05.2018

Table of Contents

List of Figures

List of Tables

Acknowledgement

First of all, I would like to express my thanks to my thesis advisor Dr. Ramona Schulz-Heddergott for the opportunity to graduate in her group, and for her patience, support, professional and personal guidance towards the end of this work. I am thankful to her for giving me every opportunity to learn and providing advice when necessary.

Furthermore, I am grateful to Prof. Matthias Dobbelstein for giving me a chance to work in his department; Institute of Molecular Oncology, Georg-August University of Göttingen.

Additionally, I would like to thank to Zainab Tayeh for her helpful advices and scientific discussions about the fascinating protein; PLK4.

I would like to thank to all lab members of Molecular Oncology for supportive, helpful and nice working environment. Especially special gratitude to Nadine Stark for teaching me every single detail of each method that I had performed for this study. Also big thanks to my office friends; Feli, Kai, Valentina and Luisa for cheerful environment, mutual support and laughs. Many thanks to Valentina again for proofreading my master thesis.

Finally, in particular I would like to thank and appreciation to my precious parents, Aysun and Hasan, and the best brother on the earth Emre, for their countless love, support and encouragement. Also, I would like to thank to my lovely friend and flatmate İdil, I can't imagine this adventure without her. Last but not least, I would like to thank to my dear Çağatay for his endless support and love throughout this journey.

Abbreviations

aa	Amino acid
Ab	Antibody
ARF	Alternative Reading Frame protein
C	Cytosine
cDNA	Complementary DNA
CHX	Cyclohexamide
CTD	C-terminal domain
CRC	Colorectal Carcinoma
CDK	Cyclin-dependent kinase
DBD	DNA binding domain
DEPC	Diethylpyrocarbonate
DMSO	Dimethyl sulfoxide
DN	Dominant negative
DNA	Deoxyribonucleic acid
dNTP	Deoxynucleoside triphosphate
DREAM	Dimerization partner, RB-like, E2F and multi-vulval class B
EDTA	Ethylenediaminetetraacetic acid
FCS	Fetal Calf Serum
For	Forward
G	Guanine
GOF	Gain of function
HSF1	Heat shock factor 1
HSP90	Heat shock protein 90
KD	Knockdown
kDa	Kilodalton
LOF	Loss of function
LOH	Loss of heterozygosity
MAPK	Mitogen-activated protein kinase
MLK3	Mixed-lineage protein kinase 3

MDM-2	Mouse double minute 2 homolog
mut	Mutant
n	Sample size
OD	Oligomerization domain
PBS	Phosphate buffer saline
PCR	Polymerase chain reaction
PLK4	Polo-like kinase 4
PRR	Proline-rich region
p-value	Probability value
qRT-PCR	Quantitative Real Time PCR
R	Purine
Rb	Retinoblastoma
Rev	Reverse
RIPA	Radioimmunoprecipitation assay buffer
RNA	Ribonucleic acid
Rpm	Revolutions per minute
RT	Reverse transcription
scr2	Scrambled siRNA #2
SDS	Sodium dodecyl sulfate
SDS-PAGE	Sodium dodecyl sulfate polyacrylamide gel electrophoresis
siRNA	Silencer RNA
TAD	Transactivation domain
Taq	*Thermus aquaticus*
Tris	Tris(hydroxymethyl)aminomethane
TBS	Tris buffered saline
TBS-T	Tris buffered saline + Tween20
TEMED	Tetramethylethylenediamine
W	Adenine/Thymidine
WHO	World Health Organization
wt	Wild type
Y	Pyrimidine

Units

sec	Second
min	Minute
h	Hour
°C	Celsius
g	Gram
l	Liter
M	Molar
m	Meter
g	Gravitational acceleration

Prefixes

n	Nano (10^{-9})
µ	Micro (10^{-6})
m	Milli (10^{-3})

Abstract

p53 activates a wide range of target genes to suppress tumorigenesis. As an important player in maintaining genome stability, p53 is able to induce cell cycle arrest, senescence and apoptosis as part of its tumor suppression activities. p53 is modified and activated upon several stress factors, e.g. DNA damage, reactive oxygen species or hypoxia.

Upon activation, p53 induces its target gene expression, e.g. cyclin-dependent kinase inhibitor 1 (p21), a major p53 target gene. p21 is responsible for cell cycle arrests by direct binding and inhibition of cyclin-dependent kinases (CDKs), which block the G1 to S transition via E2F-related gene transcription.

Previous results of our group showed that p53 is also able to regulate the stress-inducible HSF1/HSP90 (heat shock factor 1/heat shock protein 90) system, a powerful chaperone system to drive cancer. Here, p53 activation via Nutlin suppresses the phosphorylation and subsequently activation of the stress-induced transcription factor HSF1.

We hypothesized that p53 suppresses the HSF1 activity through regulation of E2F-related target genes. To test this hypothesis, we analysed possible mechanisms between p53-p21-CDK-E2F axis and HSF1 activity in colorectal cancer. E2F-regulated genes such as CDK1, CDK2, PLK4 and MLK3 were analysed as possible candidates regulating HSF1 activity. We found that CDK1 and CDK2 have contrary effects on HSF1 activity since depletion of these two-kinase causes increased level of HSF1. Additionally, we identified that PLK4 is a HSP90 client however its effect on HSF1 activity remains elusive. As a strong candidate for p53-E2F-mediated HSF1 regulation, we showed that MLK3 is activating the HSF1 system via MAPK kinase MEK pathway.

Zusammenfassung

p53 ist einer der wichtigsten Tumorsuppressoren und unterbindet die Entstehung und Entwicklung von Tumoren durch z.B. Regulationen des Zellzyklus oder DNA Reparaturmechanismen. Stark geschädigte oder gestresste Zellen werden durch p53 in den Zelltod geschickt. p53 selbst wird durch eine Vielzahl von Faktoren aktiviert, u.a. DNA Schäden, Anhäufung von reaktiven Sauerstoff oder auch Sauerstoff- und Nährstoffmangel. Nach Stressinduktion führen verschiedenste posttranslationelle Modifikationen an p53 und seinen negativen Regulator MDM2 zur Zerstörung des p53-MDM2 Komplexes und somit zur Aktivierung von p53 Zielgenexpression.

Der cyclin-dependent kinase (CDK) inhibitor 1 (p21) ist ein Hauptzielgen von p53 und reguliert den Zellzyklus. Durch Bindung von p21 an CDKs, werden diese inhibiert, was wiederum zur Verminderung von E2F-regulierten Zielgenen führt. Ein Wegfall von E2F Zielgenen verhindert den G1 zu S Übergang im Zellzyklus. Letztendlich führt eine p21 Expression durch p53 zu einem G1/S Arrest in der Zelle.

Bisherige Ergebnisse unserer Arbeitsgruppe haben zudem gezeigt, das p53 das stress-induzierte HSF1-HSP90 System in Darmkrebs reguliert, ein überaus wirkungsvolles tumorförderndes System. Eine p53-p21 Aktivierung führt zum Verlust einer aktivierenden Phosphorylierung vom Transkriptionsfaktor HSF1 (heat-shock factor 1), welches letztendlich zum Verlust der HSF1 Zielgenexpression beiträgt.

Wir vermuten, dass p53 über ein E2F Zielgen oder dessen downstream Ziele die HSF1 Phosphorylierung regulieren kann. Daher wurde innerhalb dieser Arbeit nach einer Verbindung zwischen dem p53-p21-CDK-E2F Weg und der HSF1 Aktivität gesucht. E2F-regulierte Gene wie CDK1, CDK2 und PLK4, sowie MLK3 wurden getestet. Überraschenderweise scheinen CDK1 und CDK2 die HSF1 Aktivität negativ zu regulieren, d.h. eine Verringerung der CDK1 oder CDK2 Level führte zu einer Erhöhung der HSF1 Phosphorylierung. Das E2F Zielgen PLK4 erwies sich auf Proteinebene als überaus schwach regulierter Kandidat, da das PLK4 Protein durch Hsp90 stabilisiert wird und zudem kein großer Einfluss auf die HSF1 Aktivität festgestellt wurde.

Letztendlich identifizierten wir, dass MLK3, als bisher unbekanntes E2F Zielgen, einen großen Einfluß auf die HSF1 Phosphorylierung und HSF1 Zielgenexpression hat.

Zusammenfassend lässt sich sagen, dass p53 über einen p21-CDK-E2F-MLK3 Weg die stress-induzierte MAPK Kinasen MEK1/2 inhibiert, was zum Verlust der HSF1 Aktivität führt.

1. Introduction

1.1 The p53 pathway

Four decades ago, a 53 kDa protein that can interact with the viral SV40 T-antigen and is frequently detected at high levels in cancer cells, was discovered and triggered the field of p53 research (Brosh & Rotter, 2009). In these preliminary studies, p53 was mistakenly considered to be a tumour antigen since it had been identified in oncogenic viral protein, strongly suggesting that it was an oncogene with transforming capabilities. Whereas, it has since become known as the most important tumor suppressor and "the guardian of the genome" because of its role in conserving stability by preventing genome mutation (Levine & Oren, 2009). p53 is a stress response protein that regulates a large number of signalling pathways in response to a variety of cellular stress, such as oncogene activation and DNA damage (Brosh & Rotter, 2009).

1.1.1 The structure of p53

The *TP53* gene that resides on chromosome 17p13.1 and encodes the p53 protein, is the most frequent target for mutation in human cancer, with more than half of all tumors exhibiting mutations at this locus (Petitjean et al., 2007; Vogelstein, Lane, & Levine, 2000). As shown in Figure 1, p53 has a primary function as tetrameric transcription factor and it bears an amino-terminal transactivation domain, a folded core DNA-binding domain, flanked by carboxy terminal, tetramerization and regulatory domains (Joerger & Fersht, 2010).

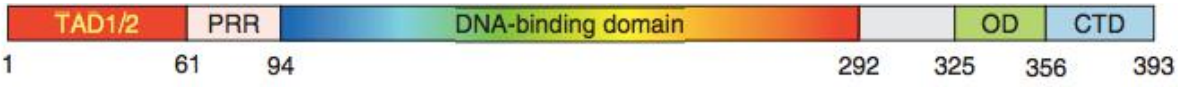

Figure 1: Domain structure of p53. p53 is composed of 393 amino acid. It contains an unfolded amino-terminal transactivation domain (TAD), subdivided into two subdomains called TAD1 and TAD2, followed by a proline-rich region (PRR). The DNA-binding domain and the oligomerization domain are connected by a flexible linker region. The C- terminal domain (CTD) is also intrinsically disordered as the TAD region. The structure of the DNA-binding domain (DBD) is shown as a ribbon representation and colored with a rainbow gradient from amino (red) to carboxyl (blue) terminus (modified from Freed-Pastor & Prives, 2012).

p53 protein consists of 393 amino acid (aa). The transcriptional activation domain (TAD1) of p53 has been mapped to the amino terminal residues 1-42 (Unger, Nau, Segal, & Minna, 1992), the proline-rich domain which also harbours the second transactivation domain (TAD2), resides in residues 40 -92, the DNA-binding domain (DBD) of p53 resides in residues 101-306, the oligomerization domain (OD) resides in residues 307-355 and also contains a nuclear export signal, and the C-terminal regulatory domain resides in residues 356-393 that also contains three nuclear localization signals (Freed-Pastor & Prives, 2012). The central core of the p53 protein resides in the DBD, which consists of several arginine amino acids that are essential for stabilizing the hairpin conformation and thus positioning for DNA binding The sequences of this domain provide p53 to recognize the elements within the promoters of target genes and therefore their transcription is initiated (Joerger & Fersht, 2010).

1.1.2 Regulation of p53

The activation of p53 upon several stress factors such as oncogene activation, DNA damage, hypoxia and nutrient deprivation, is regulated by three rate-limiting steps; which are stabilization induced by ATM and ATR mediated phosphorylation, sequence-specific DNA binding and target gene activation by recruiting the general transcriptional machinery (Kruse & Gu, 2009). During homeostasis in unstressed cells, p53 activity is negatively regulated by binding to mouse double minute 2 homolog (MDM-2) (Figure 2). MDM-2 is an E3 ligase and promotes p53 degradation by the nuclear and cytoplasmic 26S proteasomes via the ubiquitin-dependent pathway (Y. Haupt, Maya, Kazaz, & Oren, 1997; Shirangi, Zaika, & Moll, 2002). MDM-2 expression is regulated by two promoters, P1 and P2. The P1 promoter is active at basal constitutive levels in most cells (Mendrysa & Perry, 2000). MDM-2 transcripts that are derived from P1 promoter are p53 independent. p53 binds the MDM-2 P2 promoter which leads to expression of p53-induced MDM-2 forming the negative feedback loop (Dimitriadi et al., 2008).

Thus, MDM-2 is the main negative regulator of p53 in most of the p53 wild-type tumours. By blocking the interaction between p53 and MDM-2, p53 accumulates and leads to target gene expression which induce growth arrest and/or apoptosis in cancer (H. Shen & Maki, 2011).

Several mechanisms have been described to disrupt p53/MDM-2 complex such as; phosphorylation of p53 to abolish the MDM-2 binding sites or inhibition of MDM-2 by alternative reading frame (ARF) protein (Roxburgh et al., 2012). Thus, p53 can escape from the degradation-promoting effects of MDM-2 (Moll & Petrenko, 2003).

The first potential and selective small MDM-2 antagonist called Nutlin-3 was identified from a cis-imidazoline compound by using a biochemical screening method (Vassilev et al., 2004). As a principle, Nutlin-3 occupies the p53 binding pocket of MDM-2 by mimicking the molecular interactions of the necessary amino acid residues from p53 (H. Shen & Maki, 2011). It has been shown that Nutlin-3 is the most specific inhibitor of p53-MDM-2 interaction in the cellular context, leading to p53 stabilization and activation of the p53-p21 pathway (Tovar et al., 2006).

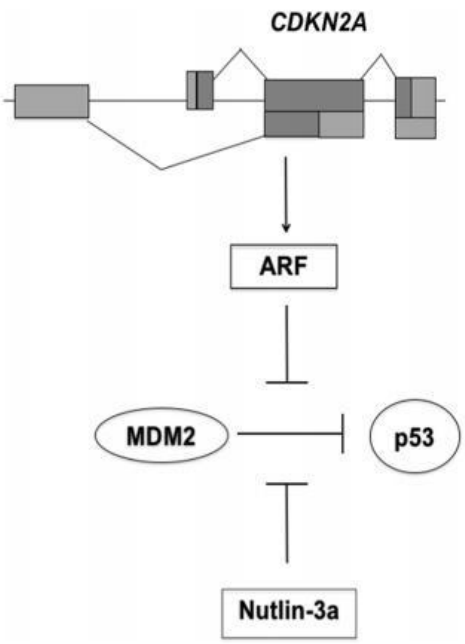

Figure 2: Model for p53 activation. The MDM-2 inhibitor ARF (encoded by *CDKN2A*) is induced upon several stresses such as DNA damage. ARF binds and inhibits MDM-2 which leads to the release of p53. Nutlin is a chemical small-compound which mimics MDM-2 inhibitor (modified from Trino et al., 2016).

1.1.3 p53 as transcription factor

p53 functions as a homotetramer in cells, binding to p53 response elements composed of two decamers separated by a spacer of 0-14 random nucleotides (5'-RRRCWWGYYY-spacer-RRRCWWGYYY-3') (El-Deiry, Kern, Pietenpol, Kinzler, & Vogelstein, 1992; Funk, Pak, Karas, Wright, & Shay, 1992; Riley, Sontag, Chen, & Levine, 2008). Several genes have been shown to be transcriptional targets of p53. Thereby p53 acts as inducer and is not able to directly repress genes (Freed-Pastor & Prives, 2012). The products of p53 target genes regulate the downstream cellular events of p53 activation such as cell cycle arrest, senescence, apoptosis and metabolic processes (Prives & Hall, 1999; Vousden & Lu, 2002; Vousden & Prives, 2009; Vousden & Ryan, 2009).

1.1.4 The target genes of p53 and their function

p53 activates a wide range of target genes to suppress tumorigenesis. According to many studies, p53 is able to induce cell cycle arrest senescence and apoptosis as part of its tumor suppression activity (Kaiser & Attardi, 2017). Activated p53 can bind to consensus sites in the genome and induce transcription of target genes to prevent tumorigenesis (Bieging, Mello, & Attardi, 2014; Vousden & Prives, 2009). Additionally, p53 has transactivation-independent functions such as apoptosis through mitochondrial membrane permeabilization (Mihara et al., 2003). High-confidence p53 target genes function in multiple processes containing, but not limited to, cell cycle arrest, DNA repair, apoptosis, metabolism, autophagy, translation control and feedback mechanism (Figure 3).

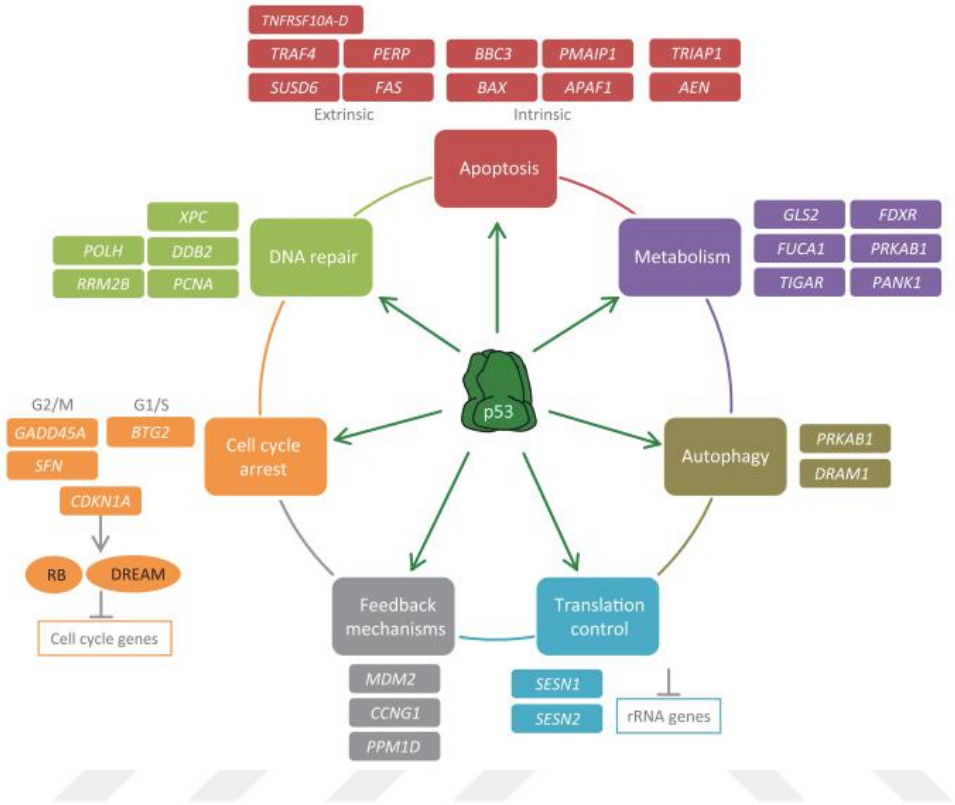

Figure 3: Main functions of p53 target genes. Target genes that are directly activated by p53 have multiple functions. In response to DNA damage, p53 is activated and p53-induced proteins can lead to cell cycle arrest, DNA repair, apoptosis, and are also involved in metabolism, autophagy, translation control and feedback mechanism. However, the function of p53 target genes are not restricted to the represented processes, but they are involved in several other cellular process. The genes are colored corresponding to their functions in the figure (modified from Fischer, 2017).

Among these p53 target genes, *CDKN1A* (*p21 / WAF1 / CIP1*) which encodes a cyclin-dependent kinase inhibitor is responsible for the cell cycle arrest and activates the cell cycle check points upon e.g. DNA damage. Cell cycle check points are the control mechanisms that ensure proper cell division of a cell. In case of DNA damage these check points allow cells to halt cell cycle progression and resolve any damage which could promote cancer development (el-Deiry et al., 1993). p21 is involved in both G1/S and G2/M cell cycle checkpoints (Agarwal, Agarwal, Taylor, & Stark, 1995; Kastan, Onyekwere, Sidransky, Vogelstein, & Craig, 1991; Lin, Shields, Ullrich, Appella, & Mercer, 1992). The p21 protein directly binds and inhibits cyclin-dependent kinases (CDKs) which in consequence preventing the phosphorylation of retinoblastoma protein (RB).

When E2F is in a complex with unphosphorylated RB, E2F transactivation is physically blocked. This in turn inhibits the gene expression required for entry to the S phase and DNA synthesis (Figure 4).

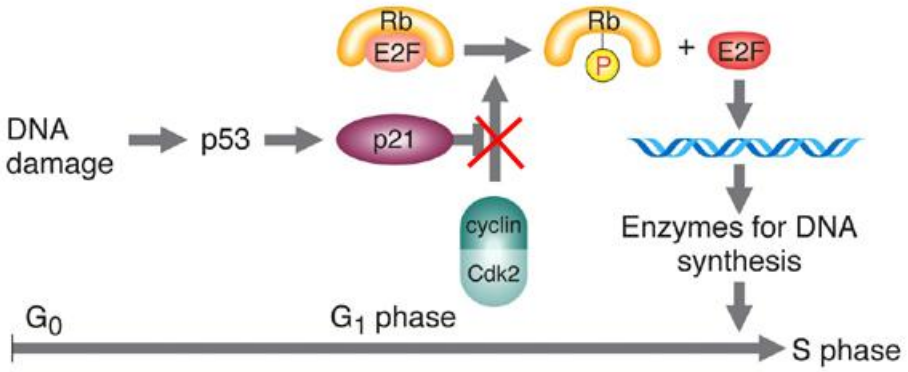

Figure 4: Schematic representation of p21 dependent E2F regulation. CDKs phosphorylate RB protein which leads to release of E2F and E2F target gene expression. E2F expressed genes promote the entry into S phase (modified from Krempels, n.d.).

1.2 The E2F system: RB – dependent E2F functions versus DREAM complex

In response to p53 activation and p21 expression, the E2F activity can be regulated via two different axes. The E2F system include large group of genes that encodes a family of transcription factors that are involved in cell cycle regulation and DNA synthesis. E2F family members have been categorized into subfamilies on the basis of transcriptional activity. Importantly, E2F has to be distinguished between RB-dependent and DREAM (dimerization partner, RB-like, E2F and MuvB)-related E2Fs. Firstly, RB-dependent E2Fs are activator transcriptional factors (E2F1-3) (Bertoli, Skotheim, & De Bruin, 2013). The mechanism is demonstrated in Figure 4. Secondly, RB-like DREAM-related E2Fs have repressor activity such as E2F4 and E2F5. At the end, all genes which are down-regulated by p53 are indirect p53-regulated genes through a repression of E2Fs (M. Fischer, 2017).

The DREAM complex is a master coordinator of cell cycle transcription (Litovchick et al., 2007; Sadasivam & DeCaprio, 2013; Schmit et al., 2007). Fischer and colleagues showed high confidence

maps of TP53 regulated genes from variety of cell types. They identified DREAM and RB-E2F related cell cycle genes to provide an overview of how these factors function to regulate cell cycle gene expression (Martin Fischer, Grossmann, Padi, & DeCaprio, 2016).

The stabilization and the activation of the repressive RB-related DREAM complex through p21 is shown in Figure 5. Due to the recruitment of the DREAM complex to the target gene promoters via its stabilization, indirect p53-mediated cell cycle genes are repressed (Calvisi et al., 2011; Martin Fischer, Grossmann, et al., 2016; Müller, Stangner, Schmitt, Wintsche, & Engeland, 2016). Thus, cell cycle genes downregulated by TP53 are directly bound to the DREAM complex.

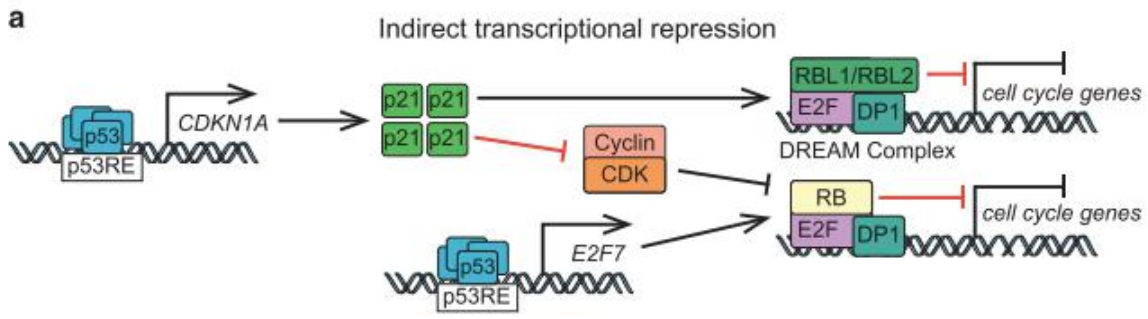

Figure 5: Mechanism of p53-dependent repression of cell cycle gene expression. p53 indirectly downregulates the E2F target gene expression by transactivation of CDKN1A which encodes p21, a CDK inhibitor, and therefore leading to transcriptional repression of cell cycle progression genes by RB-E2F4 complex and the DREAM complex(Benson et al., 2014; Martin Fischer, Quaas, Nickel, & Engeland, 2015; Martin Fischer, Quaas, Steiner, & Engeland, 2016; Quaas, Müller, & Engeland, 2012). Additionally, p53 directly activates E2F7 which is a repressive member of the E2F family (Aksoy et al., 2012; Carvajal, Hamard, Tonnessen, & Manfredi, 2012) (modified from Sullivan, Galbraith, Andrysik, & Espinosa, 2018).

Polo like kinase 4 (PLK4) and Cyclin dependent kinase 1 (CDK1) are two of the proteins that are transcriptionally regulated by the DREAM complex (Figure 6), and both have important roles in the cell cycle.

PLK4 is a master regulator of centrosome duplication and it is essential in centriole biogenesis. It has been shown that depletion of PLK4 causes centrosome duplication arrest, while overexpression of PLK4 induces centrosome over-amplification; where the both cases lead to chromosomal

instability (Archambault & Glover, 2009; Bettencourt-Dias et al., 2005). According to previous studies PLK4 is either over or under expressed in human colorectal cancer (Habedanck, Stierhof, Wilkinson, & Nigg, 2005).

In a normal dividing cell, the expression of PLK4 transcripts increases gradually from G1 to S phase and peaks during the G2 and M phases, so that the highest level is observed during mitosis (Swallow, Ko, Siddiqui, Hudson, & Dennis, 2005). Similarly, PLK4 becomes active in the S phase and its activity roughly doubles in G2 (Sillibourne & Bornens, 2010).

CDK1 functions as serine/threonine kinase and it regulates cell cycle progression by binding to its cyclin partners. The kinase activity depends on either accumulation or degradation of the cyclin during the cell cycle. In response to stress such as DNA damage, p53-p21 is activated and represses E2F-mediated CDK1 transcription.

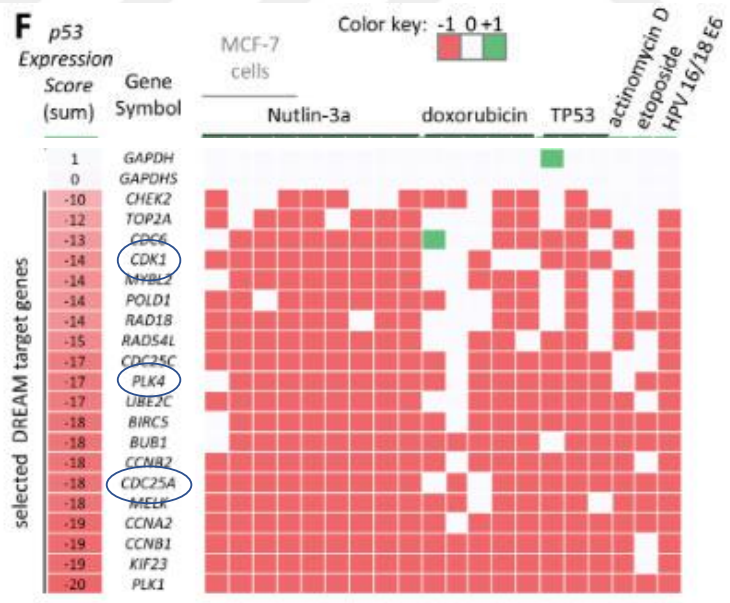

Figure 6: A heatmap representing the regulation of 20 well-established DREAM target genes. The selected genes; CDK1, PLK4 and CDC25A are the possible candidates for the stress regulation pathway (modified from Martin Fischer, Grossmann, et al., 2016).

1.3 Stress pathways

1.3.1 MAPK cascade

Stress stimuli activates specific intracellular signalling networks to regulate cell fates from survival to apoptosis (Nakamura, Saito, & Takekawa, 2013). The MAPK pathways play a key role in transduction of extracellular signals to cellular responses. This cascade system integrates signals from a diverse range of stimuli and reveal appropriate response including cellular proliferation, differentiation, development, inflammatory responses and apoptosis (W. Zhang, Liu, & Tu LIU, 2002). Figure 7 shows a very simplified overview of MAPK pathways involving a series of protein kinase cascades important for cell regulation. These cascades consist of three core protein kinases called; MAPKKK, MAPKK and MAPK (mitogen activated protein kinase). Upon a broad range of cellular stresses, mammalian cells express a large number of MAPKKK, such as MEKK1/2/3, MTK1, TAK1 and MLK1/2/3, each of them activated in response to different stimuli. When a cell is exposed to a stress, both p53 and MAPK pathways, are important determinants of cell fate (Nakamura et al., 2013).

p53-E2F-related genes are able to manage cellular stress responses to maintain genomic stability after a various kind of cellular stresses (Kruse & Gu, 2009; Vousden & Lane, 2007). Prominent stress pathways activated by p53 are the ERK, MAPK, p38 and JNK MAPK (SAPK) cascades, dependent on the cell type and cell context.

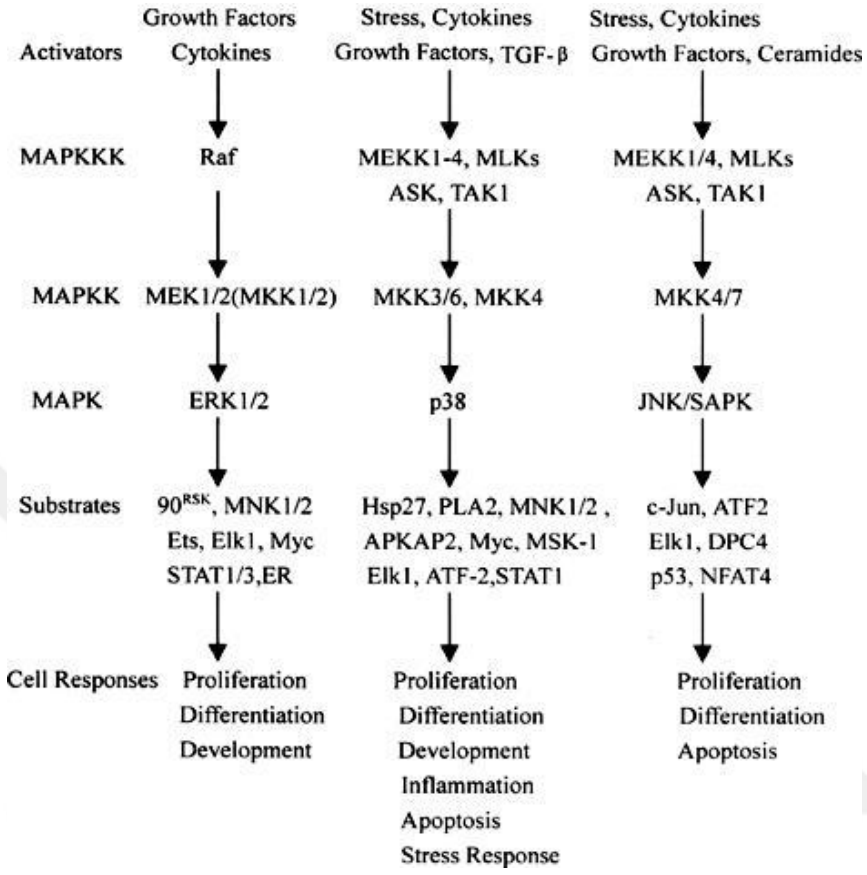

Figure 7: Major MAP kinase cascades in mammalian cells. (modified from Zhang et al., 2002)

1.3.2 The stress-inducible Heat-shock protein (HSP) machinery

Molecular chaperones assist proper folding of proteins against environmental and physiological stress and protect them from aggregation and misfolding. The chaperone function is dramatically subverted during oncogenesis to make malignant lifestyle possible (Whitesell & Lindquist, 2005). The stress-inducible HSPs level are increased in cancer cells compared to normal tissues. Cancer cells have constant stress which leads to constitutive hyper-activation of Heat Shock Factor 1 (HSF1), the master transcriptional factor of the inducible stress-response. Therefore, hyperactivated HSF1 aberrantly increases HSPs expression and cause protection of tumor prone proteins and oncogenes. Prominent clients of HSP90 can be exemplified as mutated p53, AKT, ErbB2 and Stat3.

HSF1 is the best characterized member of HSF family and it is regulated by diverse post-translational modifications (Wu, 1995). Under normal conditions, the majority of HSF1 exists in monomeric and inactive form. In response to stress conditions such as heat shock, bacterial and viral infections, proteotoxic agents or heavy metals, HSF1 is quickly converted to its transcriptionally active form by proceeding through multiple steps; these involve a transition from monomer to trimer form, a gain of DNA binding ability, nuclear accumulation and lastly posttranslational modifications (Anckar & Sistonen, 2007).

DNA-bound HSF1 is insufficient to activate transcription of *hsp* genes, which suggests that other mechanisms are required to facilitate HSF1 trans-activating competence. The transition to trimer active form of HSF1 happens concurrently with hyper-phosphorylation of serine residues which are mostly states in regulatory domain. It has been shown that phosphorylation of HSF1 at the residue of serine 326 (pSer326) by several members of the MAPK stress cascade namely; mTOR, ERK1/2 or MEK1, is required to render it transcriptionally competent (Ciocca, Arrigo, & Calderwood, 2013; Sarge, Murphy, & Morimoto, 1993).

1.4 TP53 alterations in colorectal carcinoma (CRC)

1.4.1 Colorectal carcinoma (CRC)

Colorectal carcinoma (CRC) is the development of cancer from the colon to the rectum and is a heterogeneous group of diseases with distinctive genetic and epigenetic background. More than 90% of CRCs are adenocarcinoma (International Agency for Research on Cancer, 2008). Globally more than 1 million people get CRC every year. It is the fourth most common cancer in men (after lung, prostate, and stomach cancer), and the third cause of cancer in women (after cancers of the breast and uterine cervix). CRC occurs mostly in industrialized and high resource countries in Europe, Australia, New Zealand, America and Japan. Incidence of this disease increases with age and it rarely comes across before the age of 40, except in individuals with genetic redisposition or genetic conditions such as chronic inflammatory bowel diseases. As shown in the Figure 8, the worldwide mortality is about the half of the incidence rate which is about 608 000 deaths from CRC (International Agency for Research on Cancer, 2008).

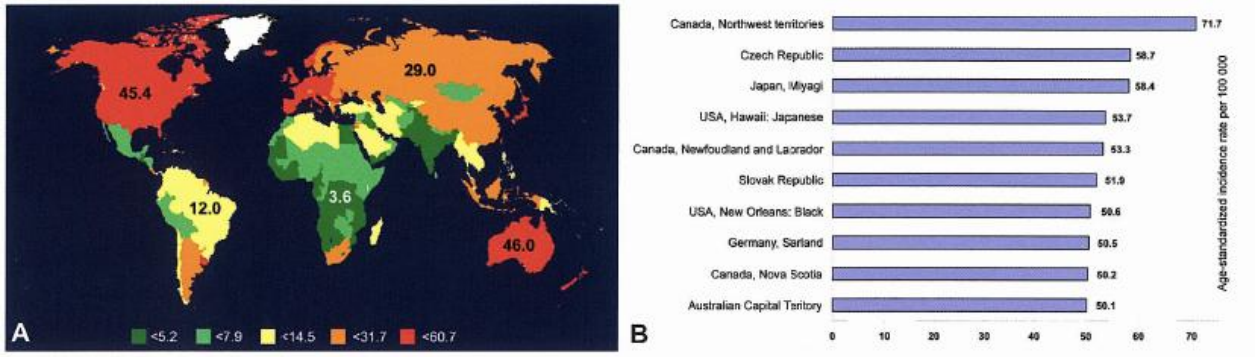

Figure 8: Worldwide annual incidence (per100 000) of cancer of the colon and rectum. A. Numbers on the map indicate regional average values and are higher in developed countries. **B.** Age-standardized incidence (per 100 000) of colorectal cancer in men in selected countries (Ferlay et al., 2015).

Populations with a "western-type" diet which contains highly caloric foods, combined with sedentary lifestyle have high incidence of CRC. According to etiological studies about CRC, it has been shown that obesity, meat consumption, smoking and alcohol consumption are most important avoidable risk factors (Koo, Mang, & Ho, 1997; Soliman et al., 1999). Chronic inflammatory bowel diseases are also etiological factors for CRC; these diseases are consisting of ulcerative colitis, Crohn diseases, Schistosoma mansoni infection.

1.4.2 Molecular mechanisms of CRC

Colorectal tumors arise as a consequence of mutational activation of oncogenes combined with mutational inactivation of tumor suppressor genes. Chromosomal abnormalities causing aneuploidy, deletions, duplications and increased amount of DNA content has been identified in colorectal tumors. Almost all of CRC patients have APC (>90%) mutation which is followed by KRAS mutation and TP53 mutation (Figure 9). Alternatively, to KRAS mutation some tumorigenesis has BRAF mutation. Mutations in PIK3CA occurred in 25% of colon tumors and this mutation has been reported as late event. TP53 mutation is important at late stage where the tumor is transforming from adenoma to carcinoma.

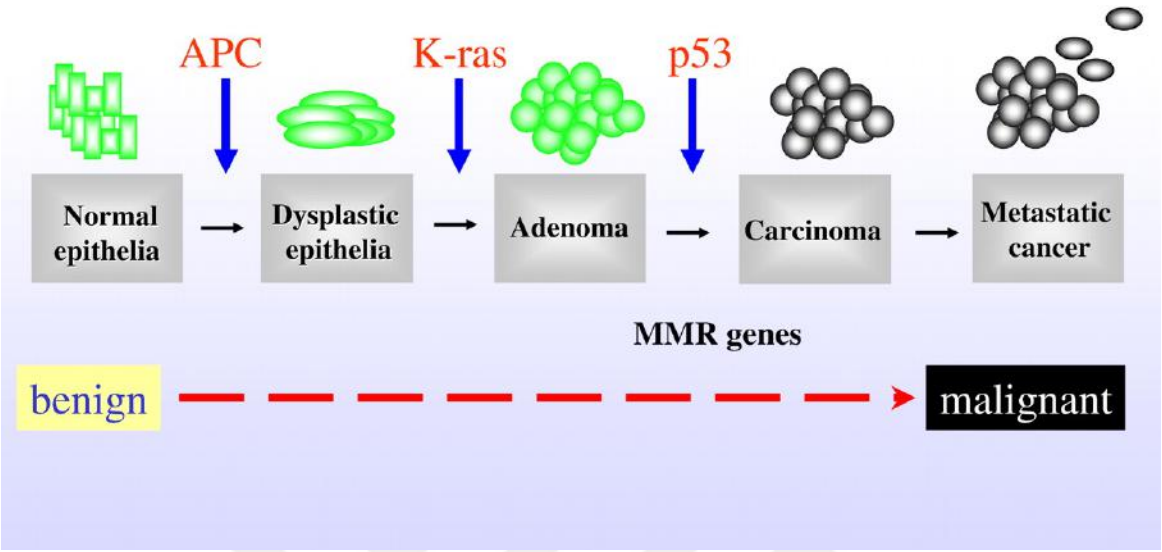

Figure 9: A model for genetic alterations required for progression from adenoma to carcinoma in the development of CRC. The proposed order of mutations in APC, K-Ras and p53 is demonstrated (modified from Smith et al., 2002).

1.4.3 Alterations of TP53 in CRC

In half of the human cancers, *TP53* tumor suppressor functions are completely eliminated, implying its important role in inhibiting cancer development. According to The Cancer Genome Atlas (TCGA) data, it has been shown that tumors with mutated *TP53* have a different gene expression profile compared to tumors that harbour wild-type *TP53* alleles. The majority of CRCs demolish wtp53 function by mutation of one or both *TP53* alleles (76%) (Figure 10). Thereby, 52% of the tumors completely lose p53 functions via p53 loss-of-heterozygosity (LOH) (last two panels of Figure 10).

Mutations of p53 are frequently followed by LOH during the tumor progression which suggests that a selective force is going to inactivate the remaining wtp53 allele (Brosh & Rotter, 2009).

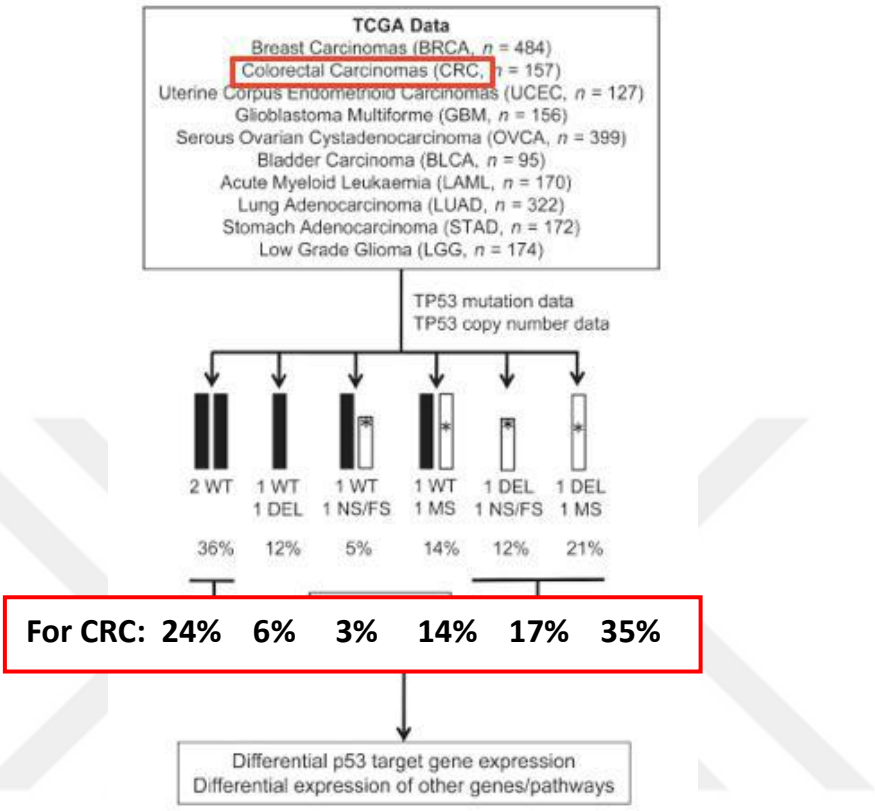

Figure 10: Gene alterations based on six different TP53 allele categories. The percentage of each TP53 allele for CRC has been represented in red box. The copy number data of ten TCGA cancer types are also shown to compare gene expression patterns based on different TP53 alleles (modified from Parikh et al., 2014). The scheme represents six categories of *TP53* allele which are diploid WT, haploid WT (WT + DEL), TP53 nonsense frame shift, or splice site mutation and diploid (WT + NS/FS), TP53 missense mutation and diploid (WT + MS), TP53 nonsense/frameshift/splice site mutation allele and haploid (deletion + NS/FS) and TP53 missense mutation allele and haploid (DEL + MS).

However, unlike most of tumor suppressor genes which are inactivated as a consequence of deletion or truncation, most mutations in p53 are missense mutations (misp53) that lead to amino acid substitution in the context of the full-length protein.

Missense mutations do not only lose their wild-type function (LOF) but gain completely new function (GOF) such as invasion, metastasis or chemoresistancies (Figure 11). Missense p53 mutants with high frequency are called “hot spot” mutants (Freed-Pastor & Prives, 2012).

Importantly, a prerequisite for misp53 GOF activity that promote malignant progression is their constitutive stabilization. Misp53 stabilization strongly depends on the HSP chaperone machinery which is significantly upregulated in cancer compared to normal tissues, protects mutp53 from degradation (E. M. Alexandrova et al., 2015).

A second major misp53 stabilization determinant in tumors that are initially p53 heterozygous (mut/wt) is p53's LOH (E. M. Alexandrova et al., 2017). In breast carcinomas and sarcomas, it was shown that wtp53 allele exerts a repressive function regarding mutp53 stabilization in vivo. In mouse tumors with high frequency of p53 LOH, mutp53 protein was stabilized (94% of cases) and GOF manifested. Conversely, in mouse tumors with low frequency of p53 LOH, mutp53 was not stabilized (80% of cases) and GOF was not observed (E. M. Alexandrova et al., 2017). In this study, how wtp53 mediates this selective pressure remains elusive.

Further, human genomic databases show a high degree of p53 LOH in all examined tumor types that carry p53 missense mutations. Thus, p53 LOH is a critical prerequisite for mutp53 stabilization leading to GOF activity in vivo. This again arises the question whether the remaining wtp53 allele enforces a selective pressure to be inactivated by LOH.

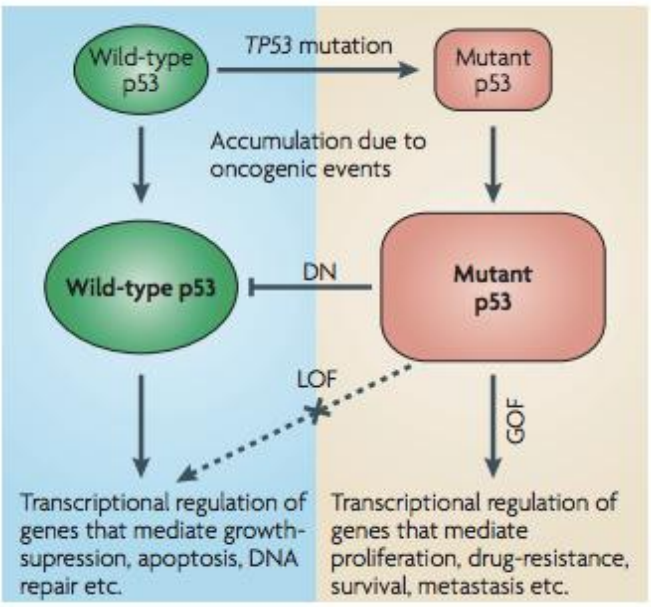

Figure 11: Functional impact of *TP53* mutations. *TP53* is inactivated by single monoallelic missense mutations, readily detected in human tumors. Beside loss of p53 function (LOF),

missense mutants can acquire new functions (GOF). A prerequisite of mutp53 GOF is the deletion of the second wtp53 (loss-of-heterozygosity) which subsequent stabilization of the misp53 protein. If the second wtp53 allele is not depleted by LOH, the mutated allele/protein can exert a dominant-negative (DN) effect over the wtp53 protein. Newest studies have shown that a remaining wtp53 allele/protein is also able to exert a dominant-positive effect over the mutated allele/protein, leading to residual p53 transcriptional activity (not shown in this overview) (modified from Brosh & Rotter, 2009).

1.5 Previous results

Previous results of our group showed that misp53 stabilization also depends on the loss of both wtp53 alleles in colorectal cancer (personal communication of unpublished results) (Figure 12). In a colorectal cancer mouse model (AOM/DSS model), misp53 stabilization only occur in tumors with a mutp53/p53null situation. The existence of one wtp53 allele (mutp53/wtp53) strongly prevents the accumulation of the mutp53 protein. Since, the HSF1-HSP90 axis is one of the major determinant of mutant p53 stability, we asked the questions whether the remaining wtp53 allele in mutp53/wtp53 situation might regulate the HSF1-HSP90 system thus preventing the stabilization of mutant p53.

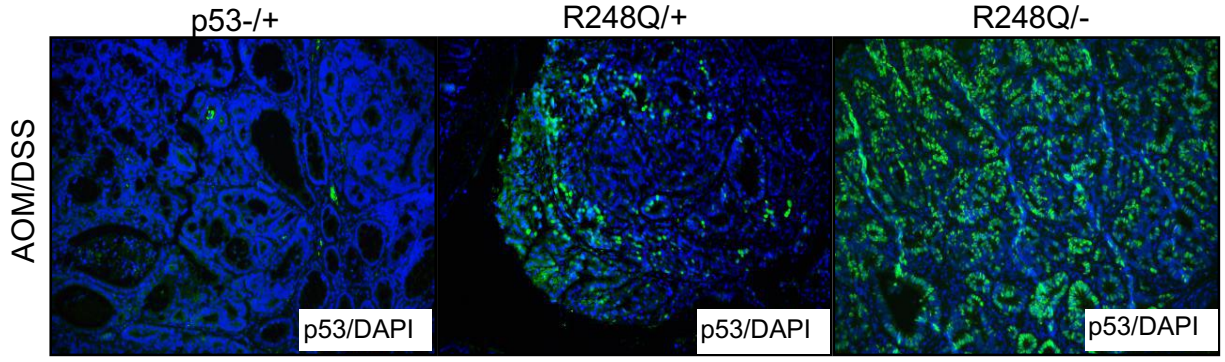

Figure 12: Immunofluorescence staining reveals that alterations in both wtp53 allele induces misp53 stabilization. (unpublished result from Ramona Schulz-Heddergott)

1.6 Aim of the study

Regarding to the observed dependency of mutp53 protein stability on p53 LOH, the question arises whether the HSF1 system is regulated by wtp53. To answer this question, wtp53-containing CRC cell lines; RKO, HCT116 and LS174T were treated with Nutlin-3a, a well-known p53 activator through inhibition of MDM-2 leading to disruption of p53-MDM-2 interaction. And indeed, Nutlin-3a represses the HSF1 response via decrease of HSF1 phosphorylation level and HSF1 target gene expression. The aim of this study is to identify the molecular mechanism of wtp53-mediated HSF1 repression.

2. Materials

2.1 Equipment

Table 1: List of equipment

Equipment	Company
Balance	Acculab, Sartorius, Göttingen, Germany
Centrifuge 5417C	Eppendorf, Hamburg, Germany
Centrifuge 5417R	Eppendorf, Hamburg, Germany
DNA engine peltier Thermal Cycler Chrome 4	BioRad, Hercules, USA
Hot plate	Thermo Scientific, Waltham, USA
Ice machine *B100*	Ziegra, Isernhagen, Germany
Incubator for cell culture, Hera Cell 150	Heraeus, Thermo Scientific, Waltham, USA
Magnet stirrer MR3001	Heidolph Instruments,SCHwabach, Germany
Mini Centrifuge GMC-060	Acculab, Sartorius, Göttingen, Germany
NanoDrop ND-1000 Spectrophotometer	Thermo Scientific, Waltham, USA
Neubauer counting chamber, Improved	Brand GmbH & Co. KG
PCR machine Thermocycler T personal	Biometra
pH-meter WTW-720 InoLab Series	WTW GmbH
Pipettes "Research" (2.5µL, 20µL, 200µL and 1000µL)	Eppendorf, Hamburg, Germany
SDS-PAGE-Chamber MiniVE	GE Healthcare, Little Chalfolt, UK
Thermal cycler	Bio Rad Laboratories
Thermomixer Comfort	Eppendorf, Hamburg, Germany
UV system	Intas Science Imaging Instruments
Vortex Genie 2	Scientific industries, Bohemia, NY, USA
Western transfer chamber (wet blot) "MiniVE Blotter"	GE Healthcare, Little Chalfolt, UK

2.2 Consumables

Table 2: List of consumables

Consumables	Company
Cell culture dishes Cellstar	Sarstedt, Nümbrecht, Germany
Cell scraper 16cm	Sarstedt, Nümbrecht, Germany
Filtertips "Biosphere®" (20µL, 200µL and 1000µL)	Sarstedt, Nümbrecht, Germany
Multiply PCR Microtube strip (8 x 0.2 ml)	Sarstedt, Nümbrecht, Germany
Nitrocellulose protran transfer membrane BA83	GE Healthcare, Little Chalfont, UK
Pipets, serological (5 mL/10 mL/25 mL)	Sarstedt, Nümbrecht, Germany
Reaction tubes (1,5 mL/2 mL)	Sarstedt, Nümbrecht, Germany
Sealing adhesive Clear seals for qPCR plates	4titude, Berlin, Germany
Sterile filter (0.2µm, 0.45µm)	Sartorius, Göttingen, Germany
Syringes (1mL/10 mL/20 mL)	Norm-Ject, Tuttlingen, Germanys
Tube, 15mL and 50mL, sterile	Greiner, Frickenhausen, Germany
Whatman paper	Whatman, Dassel, Germany

2.3 Chemicals, kits and enzymes

Table 3: List of chemicals, kits and enzymes

Chemicals & Kits	Company
Acetic Acid	Carl Roth, Karlsruhe, Germany
Acrylamide, 30%	Carl Roth, Karlsruhe, Germany
Albumin Fraction V (BSA)	Carl Roth, Karlsruhe, Germany
Agarose Standard	Carl Roth, Karlsruhe, Germany
Ammonium persulphate (APS)	Carl Roth, Karlsruhe, Germany
Ammonium sulphate	Carl Roth, Karlsruhe, Germany
BCA-Proteinassay kit	Thermo Fisher Scientific, Waltham, USA

$CaCl_2$	Carl Roth, Karlsruhe, Germany
Clarity Max^{TM} Western ECL Substrate	Bio-Rad, Hercules, USA
Immobilion Western Chemiluminescent HRP substrate	Merck Millipore, Darmstadt, Germany
Complete mini protease inhibitor, EDTA free	Carl Roth, Karlsruhe, Germany
DEPC (nuclease free) water	Ambion, Life Technologies, Thermo Fisher Scientific, Waltham, USA
dNTPs for qPCR	Primetech, Zug, Switzerland
D-Trehalose	USB Corporation
Dulbecco's Modified Eagle Medium (DMEM)	Gibco, Life Technologies, Thermo Fisher Scientific, Waltham, USA
Ethanol 99.9%	Th. Geyer, Renningen, Germany
Fetal bovine serum (FBS)	Invitrogen, Thermo Fisher Scientific, Waltham, USA
Isopropanol	Th. Geyer, Renningen, Germany
KCl	Carl Roth, Karlsruhe, Germany
KH_2PO_4	Carl Roth, Karlsruhe, Germany
L-Glutamine	Invitrogen, Thermo Fisher Scientific, Waltham, USA
Milk powder	Carl Roth, Karlsruhe, Germany
$MgCl_2$	Carl Roth, Karlsruhe, Germany
M-MuLV reverse transcriptase	New England Biolabs, Frankfurt, Germany
M-MuLV reverse transcriptase reaction buffer 10x	New England Biolabs, Frankfurt, Germany
Na_2HPO_4	Carl Roth, Karlsruhe, Germany
NaCl	Carl Roth, Karlsruhe, Germany
Nuclease free water	Thermo Fisher Scientific, Waltham, USA
2- Propanol	Carl Roth, Karlsruhe, Germany
Oligo $dT_{23}VN$	Metabion, Steinkirchen, Germany
Page ruler prestained protein marker	Thermo Fisher Scientific, Waltham, USA

Phusion HF-Buffer, 5x	Thermo Fisher Scientific, Waltham, USA
Phusion DNA Polymerase	Thermo Fisher Scientific, Waltham, USA
RNAse inhibitor	New England Biolabs, Frankfurt, Germany
Sodium dodecylsulfate(SDS)	Carl Roth, Karlsruhe, Germany
SybrGreen	Thermo Fisher Scientific, Waltham, USA
Taq-polymerase (20 U/ml)	Primetech, Zug, Switzerland
TEMED (N,N,N',N'-tetramethylethylenediamine)	Carl Roth, Karlsruhe, Germany
Triton-X-100	AppliChem, Darmstadt, Germany
Trizol	Thermo Fisher Scientific, Waltham, USA
Trypsin	Thermo Fisher Scientific, Waltham, USA
Tween 20	AppliChem, Darmstadt, Germany
Urea	Carl Roth, Karlsruhe, Germany

2.4 Buffers and solutions

Table 4: List of buffers and solutions

Buffers and Solutions	Compositions
10x qPCR mix:	1.5M Tris-HCl pH 8.8 1M (NH4)2SO4 10% Tween-20
2x qPCR Master-Mix:	1x qPCR mix 10x 3mM Trehalose in 10mM Tris 0.25% Triton X-100 1:80.000 SYBR Green 0.2mM dNTP 20U/mL Taq Polymerase
5% milk solution:	5% Skimmed milk powder in PBS
Freezing medium:	10% DMSO, 20% DMEM and 70% FCS

Laemmli buffer (6x):	0.35 M tris pH 6.8 30% glycerin (v/v) 10%SDS (w/v) 9.3% Dithiothreitol (DTT) (w/v) 0.02% bromphenol blue (w/v)
1x Cell Lysis Buffer:	20mM Tris/HCl (pH 7.5) 150mM NaCl 1mM Na2EDTA (pH 8.0) 1mM EGTA (pH 8.0) 200µL lysis buffer mastermix 10µL protein kinase K 50µL 10% SDS
10x PBS (Phosphate Buffered Saline):	236.9 mM NaCl 2.7 mM KCl 8.1 mM Na2HPO4 1.1 mM MgCl2 1.5 mM KH2PO4 1.2 mM CaCl2
1x TBS-T:	100mL 10x TBS 0.04% Tween 20 Up to 1L ddH2O
RIPA lysis buffer:	20mM Tris-HCl (pH 7.5) 150mM NaCl 1% Triton 0.1% SDS(w/v) 1% Sodium desoxycholate (w/v) 1 tablet Complete mini protease inhibitor/25 mL 9.5mM EDTA

10x SDS running buffer:	151g Tris 720g glycine 50g SDS Up to 5L ddH2O
TAE:	40mM Tris 20mM acetic acid 1mM EDTA
Western salts (10x):	60.55g Tris 0.02% SDS 288g glycine Up to 2L ddH2O (pH 8.3)
Transfer buffer:	10%Western Salts (10x) 20% Methanol
Cell culture medium + FBS:	RPMI Medium 10% Fetal bovine serum 2mM L-glutamine 100µM ß-mercaptoethanol 1mM Sodium pyruvate

2.5 Antibodies

Table 5: List of antibodies used for immunoblot analysis

Name	Supplier	Clone / ID	Source organism	Dilution
p53	Santa Cruz	Sc-126	Mouse	1:500
MLK3	Abcam	EP1460Y	Rabbit	1:1000
PLK4	Protein Technologies	12952-1-AP	Rabbit	1:1000
Cdc2 p34 (CDK1)	Santa Cruz	Sc-54	Mouse	1:500
CDK 2	Santa Cruz	Sc-6348	Mouse	1:200
phospho-HSF1	Abcam	Ab115702	Rabbit	1:1000
phospho-MEK1/2	Santa Cruz	Sc-7995-R	Rabbit	1:500

phospho-p38	Cell Signalling	9215S	Rabbit	1:1000
β-Actin	Abcam	Ab6276	Mouse	1:10000
GAPDH	Abcam	Ab8245	Mouse	1:10000
goat anti-mouse HRP	Thermo Fisher Scientific	31430	Goat	1:10000
donkey anti-rabbit IgG-HRP	Jackson ImmunoResearch	711-036-152	Donkey	1:10000

2.6 Primers

Table 6: List of primers from Metabion for quantitative PCR (100 µM)

Primer pair target	Sequence forward primer (5'→ 3')	Sequence reverse primer (5'→ 3')
36B4	GATTGGCTACCCAACTGTTG	CAGGGGCAGCAGCCACAAA
MLK3	CACACCCCCAGCACTCAAT	CGTCTTGAGCGAGAAGCAGA
PLK4	CAAGCGGCGGGAGATTTTCA	CAGCTCTGTAGACACCAGCAA
p53	ATGGAGGAGCCGCAGTCAGATC	GGGAGCAGCCTCTGGCATTCTG
p21	TAGGCGGTTGAATGAGAGG	AAGTGGGGAGGAGGAAGTAG
CDK1	TTTTCAGAGCTTTGGGCACT	CCATTTTGCCAGAAATTCGT
Cdc25c	GTATCTGGGAGGACACATCCAGGG	CAAGTTGGTAGCCTGTTGGTTTG
HSP90aa	GCCCAGAGTGCTGAATACCC	GTGGAAGGGCTGTTTCCAGA
HSP110	ACTGCTTGTTCAAGAGGGCTGTGA	AACATCCACACCCACACACATGCT
RBBP5	AACTCAGCCAGCCCTTGAC	GGCCACATGATGGCAAAGTG
ITGB3BP	TCCCGAATCTCAGAATGCCTG	TGACAAGTTCCAGTTGTTGGAG

2.7 Oligonucleotides

Table 7: List of small interfering RNAs from Ambion (50 µM)

siRNA name	siRNA	Cat. No.	Sequence Sense	Sequence Antisense
Ctrl #2 (scrambled)	ssc2	4390847	undisclosed	undisclosed
p21 #1	s415	4390824	CAAGGAGUCAGACAUUUUAtt	UAAAAUGUCUGACUCCUUGtt
p21 #2	s416		GCACCCUAGUUCUACCUCAtt	

p21 #3	s417		CAAGGAGUCAGACAUUUUAttt	
p53 #1	s605	4390825	GUAAUCUACUGGGACGGAAtt	UUCCGUCCCAGUAGAUUACca
p53 #2	s607	4390825		
CDK1 #1	s464	4427038	GGUUAUAUCUCAUCUUUGAtt	UCAAAGAUGAGAUAUAACCtg
CDK1 #2	s465	4427038	GAAUCUUUACAGGACUAUAtt	UAUAGUCCUGUAAAGAUUCca
CDK2 #1	s205	4390824	GAGUCCCUGUUCGUACUUAttt	UAAGUACGAACAGGGACUCca
CDK2 #2	s206	4390824	CAAGAUCUCAAGAAAUUCAtt	UGAAUUUCUUGAGAUCUUGgt
MLK3 #1	s8814	4427038	CGUGAUCUCAAGUCCAACAtt	UGUUGGACUUGAGAUCACGgt
MLK3 #2	s8815	4427038	GCGUAGCUGUUAACAAGCUtt	AGCUUGUUAACAGCUACGCca
MLK3 #3	s8816	4427038	CAUGGUACCUGGAUUCAGAtt	UCUGAAUCCAGGUACCAUGtg
PLK4 #1	s21083	4427037	GGACCUUAUUCACCAGUUAtt	UAACUGGUGAAUAAGGUCCtt
PLK4 #2	s21084	4427037	GGACUUGGUCUUACAACUAtt	UAGUUGUAAGACCAAGUCCtt

2.8 Cell lines

Table 8: List of cell lines

Cell line	Origin	Mutations
HCT116 wild type	Human colorectal carcinoma	CDKN2A, CTNNB1(B-catenin) PIK3CA, RAS – (kRAS)
RKO	Human colorectal carcinoma	BRAF, PIK3CA
LS174T	Human colorectal carcinoma	CTNNB1, PI3KCA, RAS – (kRAS)

2.9 Inhibitors

Table 9: List of inhibitors

Compound name	Target	Company	Catalogue No	Concentration
Centrinone	PLK4 inhibitor	MedChem Express	HY-18682	0.2, 0.5, 1, 2µM
Nutlin-3	MDM-2 inhibitor	BOC Sciences	675576-98-4	20µM
17-AAG	HSP90 inhibitor	Calbiochem	100068	5 µM
17-DMAG	HSP90 inhibitor	Sigma-Aldrich	A 8476	5 µM
Geldanamycin	HSP90 inhibitor	Calbiochem	345805	5 µM
Cyclohexamide	Protein synthesis inhibitor	Sigma-Aldrich	C 7698	2.5 µM

2.10 Software

Table 10: List of software used to analyse the data

Technical device/method using software	Supplier
Quantitative PCR	Bio-Rad CFX Manager ™ Software
NanoDrop™	ND-1000 software, Thermo Fisher
Developer	Bio-Rad Image Lab™
ImageJ	Wayne Rasband
Microsoft Office (Excel, Powerpoint, Word)	Microsoft, Redmont, WA, USA
GraphPad Prism 5.04	GraphPad Software Inc., San Diego, CA, USA
Adobe Photoshop	Adobe Systems, San José, CA, USA

2.11 Statistical Analysis

Western blot images are quantified by using BioRad's ImageLab Software and were normalized to β-actin. The ratio was relativized by setting the control group to 1. Statistical analysis of qPCR results was performed using Microsoft Excel. Two-tailed t-test was used as a statistical test and the significances are shown in the graphs by the corresponding p-values. The threshold of significance set at $p \leq 0.05$.

3. Methods

3.1 Cell culture

Cells were cultivated at 37 °C, 5% CO_2 incubators. All methods regarding on cell culture were performed under a sterile cell culture hood with an air-flow characteristic. The cell lines listed in table 8 were supplied with complete RPMI medium which contains FBS, Pen/Strep and L-glutamine. For sub-cultivation, cells were washed with pre-warmed PBS and detached from the culture dish by incubation with 0.1% trypsin/EDTA at 37 °C for 5 minutes. After detachment, the reaction was stopped by adding complete RPMI medium. Cells were reseeded periodically at dilution 1:10 two times per week. For the experiments, cells were seeded into culture dishes at desired density.

3.2 Lipofectamine transfection with siRNA

Specially designed Lipofectamine transfection reagent is cationic-lipids formulated for the delivery of plasmid DNA, siRNA or mRNA into eukaryotic cells (Chesnoy & Huang, 2000; Hirko, Tang, & Hughes, 2003; Liu, Sekito, Špiírek, Thornton, & Butow, 2003). The basic structure of cationic lipids consists of positively charged head group and hydro carbon chains. The charged head group governs the interaction between the lipid and the phosphate backbone of the nucleic acid and facilitates DNA condensation. The positive surface charge of the liposomes mediates the interaction of the nucleic acid and the cell membrane, that allows for fusion of the liposome/nucleic acid transfection complex with the negatively charged cell membrane. Entering process of transfection complex to the cell is through endocytosis; where the cellular membrane uptakes the transfection complex by forming intracellular vesicle bound to membrane. When the transfection complex is inside the cell, must escape the endosomal pathway, diffuse through the cytoplasm and enter the nucleus for gene expression. It is thought that the cationic lipids facilitate transfection during the early steps of process by mediating DNA condensation (Invitrogen by Life Technologies, 2013).

Lipofectamine transfection was performed by 20-50pmol (0.4-1µg) of siRNA mixed with 250 µl RPMI - (without supplements) on one hand 5 µL Lipofectamine2000 was added to 250 µL RPMI

-. The tubes were incubated for 5 mins at RT. Both preparations were combined 1:1, inverted several times and incubated for 20 mins at RT. The preparation was then transferred to the cells. Transfection medium was changed after 24 hours by RPMI complete medium.

3.3 Chemical treatments

Nutlin-3 is small molecule inhibitor that specifically targets p53-Mdm3 interaction that offers a new therapeutic opportunities by enhancing cancer cell growth arrest and apoptosis (Kojima et al., 2006). Nutlin is diluted in DMSO according to manufacturer's instructions and stored as 20mM. For the experiments Nutlin was diluted in pre-warmed complete RPMI supplemented with 10% fetal bovine serum (FBS) and antibiotics. In order to initiate p53-mediated response, HCT 116 and RKO cells harbouring wtp53 were treated with 20 μM Nutlin for 24 hours.

Centrinone is a reversible inhibitor for kinase PLK4 and the treatment was performed in pre-warmed complete RPMI at the concentrations listed as table 9. For all treatments corresponding dilutions of DMSO were used as control group.

Cyclohexamide is a protein synthesis inhibitor in eukaryotes. EtOH is used to prepare stock solution. For treatments 2.5 μM cyclohexamide was used in pre-warmed complete RPMI for 8 and 24 hours.

3.4 Protein harvesting

Protein isolation was performed on ice to avoid protein degradation. To isolate proteins from cells, optionally media from each corresponding well of a 6 well plate was transferred to Eppendorf tubes or possible it could be discarded. The cells were washed with 1 mL PBS, then PBS was sucked off. Approximately 100-200 ml RIPA buffer completed with protein and phosphatase inhibitors is added on cells, the amount of lysis buffer depends on cell size. After lysis buffer added to plates, cells were scratched from the plate and transferred to appropriate wells. Cell suspension was incubated on ice for at least 1 hour, should be vortexed between whiles. Following this, cell suspensions were sonicated at higher power or 15 minutes. The

tubes were centrifuged at 13 000rpm, 4°C for 15 minutes. The protein supernatant was transferred in a new tube. Following this, protein samples were stored at -80°C.

BCA test was performed to the protein samples to make sure that the same amount of proteins would be loaded. The Pierce BCA protein assay kit (Thermo Scientific) was used according to manufacturer's instructions to measure the protein concentration so that same amount of protein samples will be loaded on a 10% SDS. Finally, all protein samples were prepared to required concentrations by RIPA buffer and 6x Laemmli buffer.

3.5 SDS-PAGE and Western blot detection

SDS-PAGE (Sodium dodecyl sulphate - polyacrylamide gel electrophoresis) is a technique which involves the denaturation of proteins with detergent SDS, and the use of an electric current to pull them through a polyacrylamide gel, a process called polyacrylamide gel electrophoresis (PAGE) (George & Urch, 2000). The SDS-PAGE method is described very firstly by Shapiro and his colleges and indicated that proteins and their subunits can be separated simply and rapidly according to their molecular weight (Shapiro, Viñuela, & V. Maizel Jr., 1967). Before electrophoresis, protein samples have to be boiled at 95°C for 5 minutes to dissolve hydrophobic regions of proteins and breaks the non-covalent ionic bonds present in proteins by SDS. By this way proteins lose their globular structures and become linearized.

SDS also coats the proteins and makes them a negatively charged which is proportional to their molecular weight. Upon application of an electric field, proteins start to migrate through the anode with different speed, depending on their mass, thereby this procedure allows precise protein separation according to mass. For SDS-PAGE system, a polyacrylamide gel is used that is divided into two parts; an upper part called "stacking" gel with large pore size whereas the bottom part called "resolving" gel with smaller pores. By supplying the electric voltage, the chloride ions where present in both gels start to migrate towards anode and pulls glycine ions in the running buffer so that they move together. Depending on their size, the loaded protein samples are going to be separated due to narrow pores in the resolving gel.

The gels used for this technique are composed of 5% stacking gel on top of a %10 resolving gel. Gels were poured into a glass plates separated with 1.5mm thick spacers. The composition of resolving and stacking gel is following.

Table 11: Composition of resolving and stacking gel

Gel	%10 Resolving gel		%5 Stacking gel	
Composition	5.3 mL	ddH_2O	4.53 mL	ddH_2O
	4.43 mL	30% acrylamide	1.13 mL	30% acrylamide
	3.3 mL	Tris-buffer pH 8.8	830 µL	Tris-buffer pH 6.8
	133.3 µL	10% SDS	66 µL	10% SDS
	133.3 µL	10% APS	66 µL	10% APS
	5.3 µL	TEMED	6.6 µL	TEMED

Firstly, the resolving gel was casted and covered by isopropanol during polymerization. After it becomes polymerized, isopropanol was discarded and let it dry for 2 minutes by evaporation. Then stacking gel was casted on top of resolving gel. When stacking gel was polymerized, gels can be directly used or stored at 4°C.

As mentioned above, protein samples prepared with RIPA buffer and Laemmli buffer were boiled at 95 °C for 5 minutes before loading. Then electrophoresis process of the proteins was conducted on the system called Amersham Biosciences. For stacking gel 80V and for the resolving gel 120 V was applied constantly.

Once the gel was run completely, the separated protein bands were transferred from gel to the nitrocellular membrane which is activated by methanol. For the transfer process, a sandwich was prepared by putting the nitrocellulose membrane onto the gel and after that this was covered by Whatman papers and sponges that were moisturized by transfer buffer in advance. The prepared sandwich was placed into the chamber and filled with cold transfer buffer. This transfer process was carried out at a constant voltage of 100 V for 120 minutes at 4 °C.

Following the transfer, the nitrocellulose membrane was blocked for 1 hour in blocking solution (%5 milk solution) at RT to degrade unspecific epitopes of interested antibodies. Thereafter, the membrane was incubated at 4 °C overnight by specific primary antibodies (table 5) to detect the proteins of interest. The next day, excess antibodies were washed off in two washing steps with TBS-T for 15 minutes at RT. Following this, the blot kept in the secondary antibody (table 5) for 1 hour at RT. Again, excess antibodies were washed off in two washing steps with blocking solution for 15 minutes at RT. After that, the signals of marked proteins were developed using the Immobilon *Western Chemoluminescent HRP Substrate* (Millipore) for strong protein signals and the SuperSignal *West Femto Maximum Sensitivity Substrate* (Thermo Scientific) for weak signals that are hard to detect. For imaging of signals, the chemoluminescence imager Chemocam HR was used.

3.6 RNA isolation

To isolate RNA from 6 cm dishes, media from each dish was transferred to a 1.5 ml tube. Cells were washed with 500 µl cold PBS which was also collected. Following this, the suspension was centrifuged at 2000rpm at 4°C for 2 minutes and supernatant was socked off. 1 mL of TRIzol was added to the cells on the plate and pipetted up and down, transferred to 1.5 mL tubes. 200µl chloroform was added, incubated at least 3 minutes at RT and the eppendorf tubes were inverted for several times. Subsequently, samples were centrifuged at 12,000g at 4°C for 15 minutes. This step helps to separate the phases (upper watery (RNA), intermediate (DNA) and lower red phenol phase (protein)). After centrifugation, 200 µL of upper aqueous phase which contains RNA was transferred into a new eppendorf tube. 500 µL of isopropanol was added to the samples and was incubated for 20 minutes at RT, inverted for several times in between. After that, samples were centrifuged at 12,000g at 4°C for 15 minutes. The supernatant was discarded, the pellet was resuspended in 1 mL 75% ethanol for washing in order to remove remaining salts. Again, the tubes were inverted for several times and after that samples were spinned down at 7600g at 4°C for 1 minute. The supernatant was carefully removed, and RNA pellet was dried shortly. Depending on pellet size, RNA pellet was resuspended in 20-50 µL DEPC-H_2O and the samples were left for shaking with open lid in a heating block at 55°C for 10-15 minutes to remove the remaining ethanol.

Then, the concentration of resuspended pellet was measured with NanoDrop (taking 2 µL) and was stored at -80°C.

3.7 Reverse transcription

Reverse transcription (RT) reaction is a technology in which RNA molecules are converted into their complementary DNA (cDNA) sequences by reverse transcriptase, followed by the amplification of the newly synthesized cDNA by using traditional PCR. RT uses RNA as a starting material. By the discovery of retroviral reverse transcriptase in the early 1970s, RT is possible. Reverse transcriptase is DNA polymerase dependent on RNA and catalysing DNA synthesis by using RNA as a template. The end product is called cDNA. Producing cDNA from RNA has many advantages such as cDNA is more stable than RNA which makes it easy to work. In RT, the starting RNA is subsequently degraded, dsDNA is produced and PCR amplification proceeds in the usual manner (Elsevier B.V., 2012).

In order to obtain complementary DNA (cDNA), 1 µg RNA was mixed with 2 µL of random hexamer primers (50 µM $dT_{23}NV$ and 15 µM random monomer primers) and 4 µL 2.5mM dNTPs. Nuclease-free water was added to each tube to make the volume to 16 µL. The samples were run at 70 °C for 5 minutes. To each sample, 4 µL of master mix which is composed by 2 µL 10x reaction buffer, 0.250 µL RNase inhibitor (20U), 0.125 µL M-MuLV Reverse Transcriptase (25 U) and 1.625 µL nuclease-free water was added. The samples were incubated at 42°C for 1 hour. The enzyme was inactivated at 95°C for 5 min. Samples were diluted by adding 130 µL nuclease-free water. They were stored at -20°C.

3.8 Quantitative Real-Time PCR (qPCR)

Quantitative real-time PCR (qPCR) is a sensitive and a rapid tool that is used to detect, characterize and quantify the nucleic acid in various application such as gene expression analysis and detection of cancer phenotyping. qPCR assays are commonly used for measurement of gene copy number or presence of mutant genes in transformed cell lines. In the case of RNA quantitation, the template is complementary (cDNA) that is obtained by reverse transcription of RNA. In combination with RT reaction and qPCR, it can be precisely quantitated changes in gene expression in response to

different environmental conditions or drug treatment by measuring the changes in cellular mRNA levels (Bio-Rad, 2018).

In qPCR florescent labelling enables the collection of data as PCR progress in contrast to conventional PCR. In dye-based qPCR, fluorescent labelling which is SYBR green dye in this case allows the quantification of the amplified DNA molecules since it will bind to all dsDNA PCR products. During each cycle, the fluorescence is measured and its signal increases proportionally by the amount of replicated DNA so that DNA is quantified in "real time" (Neidler, 2017).

Quantifying the specific gene is being studied in relation to another gene which is called normalizing gene, selected for its constant level of expression. These normalizing genes are selected from housekeeping genes since these genes have basic cellular survival which implies constitutive gene expression. Therefore, researchers can analyse the ratio of the expression of gene of interest divided by the expression of the selected housekeeping gene. The qPCR experiments had been performed by using 36B4 gene as a normalizing gene.

For each primer, the following master mix was prepared (mix for 1 sample):

- 14 µL 1x qPCR mix [2x]
- 6 µL nuclease-free water
- 1 µL 100µM primer forward (1:10)
- 1 µL 100µM primer reverse (1:10)

22 µL of this mix was added to each well of a 96 well plate for qPCR. Per well, and then 3 µL of cDNA was added, and were setup in triplicates as well as ddH_2O serves as a non-template control. The plate was covered by plastic sticky lid and spin down quickly to be loaded into qPCR thermal cycler. qPCR was performed under the following conditions:

Table 12: PCR program used for qPCR.

Temperature	Time	Step	Cycles
95°C	2 min	Taq DNA polymerase activation	1
95°C	15 s	DNA melting	35
60°C	20 s	Primer annealing	35
65°C	30 s	Extension and reading	35

Melting curve was read between 65°C and 82°C. The expression levels of genes of interest were normalized to the expression of 36B4 gene (housekeeping gene).

4. Results

4.1 E2F target genes might regulate HSF1 activity

We showed that p53 activation by Nutlin-3a (briefly Nutlin) represses the HSF1 activity (personal communication of unpublished results). Since it is well-known that Nutlin induces a strong p21 and E2F-dependent cell cycle arrest, we started to analyse the effect of E2F target genes on HSF1 regulation. E2F target genes such as Cyclin-dependent kinase 1 (CDK1), CDC25C, and E2F-associated genes such as CDK2 were selected as possible candidates. Since the E2F pathway is regulated through p53 and the p53 target gene p21, Nutlin-induced HSF1 repression was compared to simultaneous p53 and p21 depletion.

Upon transfection of HCT116 cells with p53 and p21 siRNAs for 72h followed by Nutlin treatment for the final 24h, mRNA levels of p53 and p21 were measured to check the efficiency of siRNA transfection (Fig. 13 A-C). An efficient reduction of p53 mRNA expression was seen (Fig. 13A). However, the efficiency of p21 silencing was not strong enough (Fig. 13B, C). Cells transfected with p21 siRNAs were expected to have expression level at least lower than 0.2 which was not the case in our experiment (Fig. 13B). Nutlin treated HCT116 cell were depicted in another graph since p21 expression was extremely high (Fig. 13C). Thus, p21 silencing was not sufficient to perform further experiments.

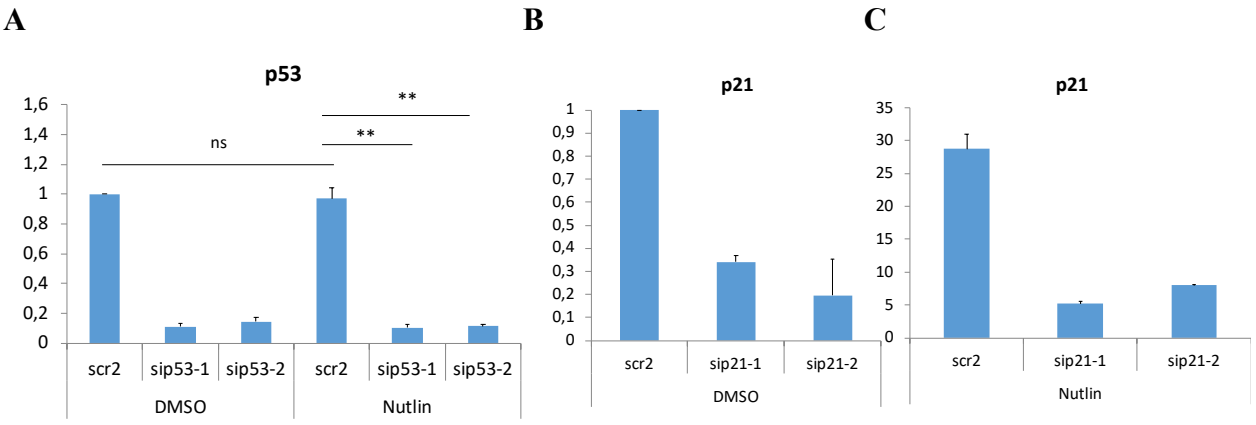

Figure 13: mRNA expression level of p53 and p21 following knockdown in HCT116 cells. A. Results of p53 qPCR level of HCT116 cells after knocking down for 72h followed by 20µM Nutlin treatment for last 24h that represents significant reduction of p53 with both siRNAs compared to controls (scr2). **B.** HCT116 cells were transfected with p21 siRNAs for 72h. **C.** HCT116 cells

transfected with p21 siRNAs and treated with Nutlin as indicated in (A). qRT-PCR results as indicated were normalized to housekeeping gene 36B4 mRNA. Relative values are given in formula (2^{-ddCT}). Error bars indicate SEM of 2 independent experiments, repeated twice, each with all in duplicates. ns: non-significant, * P≤0.05, ** P≤0.01; *** P≤0.001; **** P≤0.0001.

After validation of the efficiency of p53 depletion in HCT116 cells, E2F-mediated gene expression of CDK1, CDC25C and CDK2 was analysed via qPCRs. All analysed target genes showed a decrease in mRNA levels after Nutlin treatment (Fig. 14A-C). Importantly, the mRNA reduction was partly rescued by a simultaneously depletion of p53, showing that CDK1, CDC25C and CDK2, are p53-E2F-regulated genes. To identify possible enzymes for HSF1 regulation, the two E2F-related kinases CDK1 and CDK2 seemed to be promising candidates for further investigations.

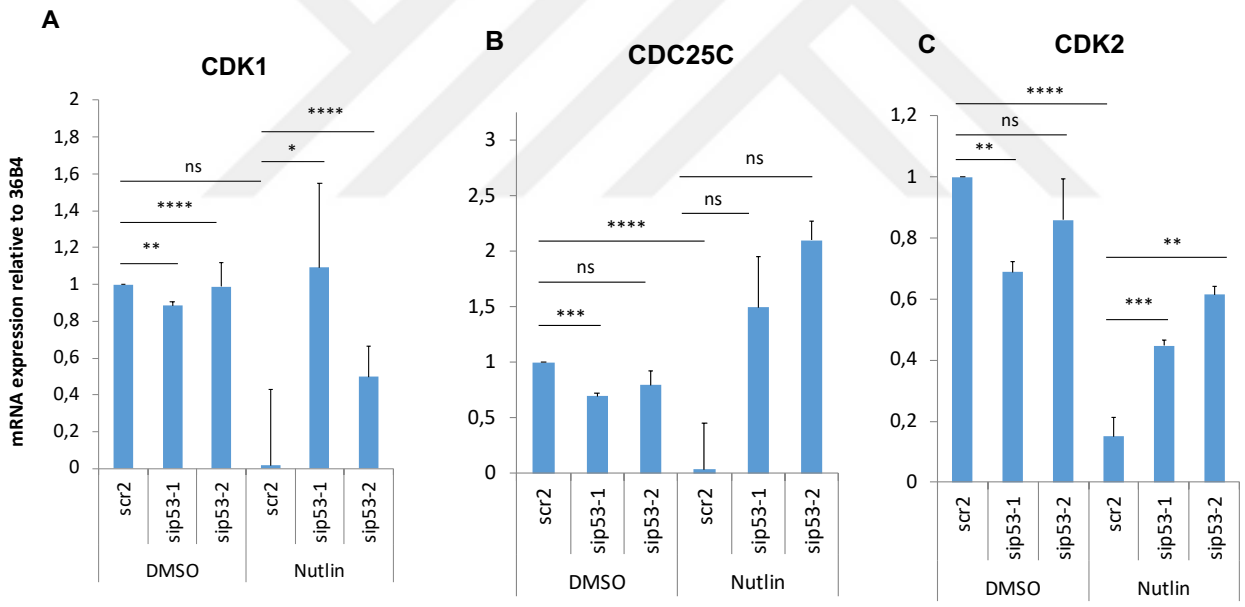

Figure 14: HCT116 cells depleted with p53 were analysed for the E2F target genes; CDK1 (A), CDC25C (B) and CDK2 (C). HCT116 cells were transfected with p53 siRNAs for 72h and treated with 20µM Nutlin for final 24h. qRT-PCR results as indicated were normalized to housekeeping gene 36B4 mRNA. Relative values are given in formula (2^{-ddCT}). Error bars indicate SEM of 2 independent experiments, repeated three times, each with all in duplicates. ns: non-significant, * P≤0.05, ** P≤0.01; *** P≤0.001; **** P≤0.0001.

4.2 Depletion of E2F-regulated genes CDK1 and CDK2 surprisingly increase HSF1 phosphorylation

HCT116 and RKO cells were transfected with siRNAs against CDK1 (siCDK1-1 and siCDK1-2) for 72h and treated with Nutlin for final 24h. p53 accumulated strongly by Nutlin treatment which shows that Nutlin treatment worked very well (Fig. 15B). The cell density of HCT116 cells is reduced and the cells seemed to have stress in the CDK1 knockdown cells compared to control cells (scr2) (Fig. 15A) since CDK1 depletion causes cell cycle arrest. The knockdown of CDK1 does not show cross depletion to other CDKs such as CDK2 (Fig. 15B). Surprisingly and against our expectations, depletion of CDK1 with or without Nutlin increases HSF1 phosphorylation. If an E2F-related kinase would directly regulate HSF1 phosphorylation, we would expect a downregulation of HSF1 phosphorylation.

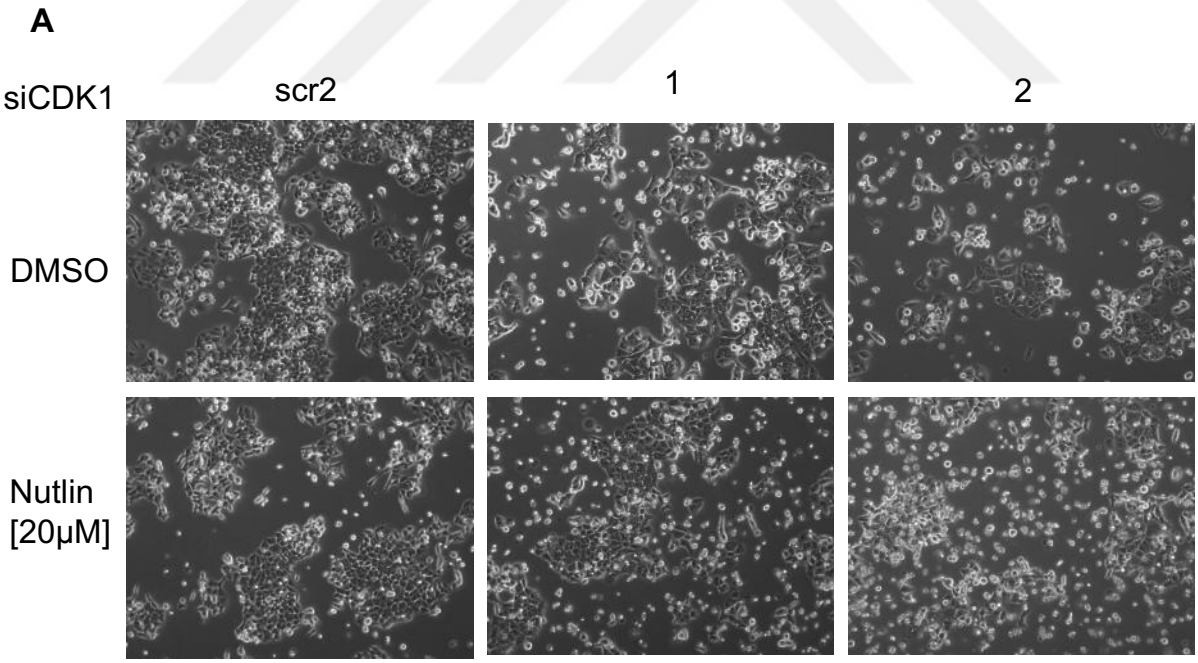

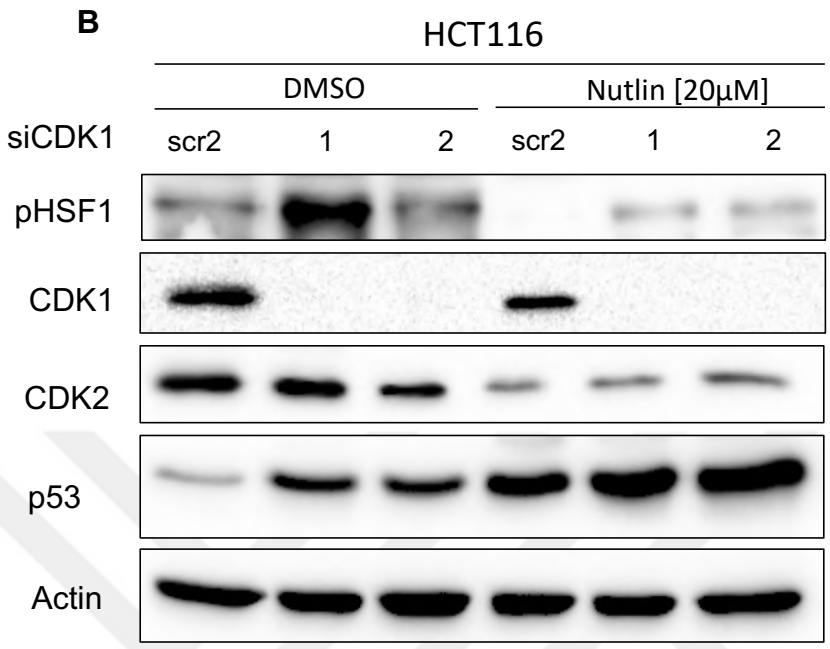

Figure 15: CDK1 depletion in HCT116 cells increases HSF1 phosphorylation. HCT116 cells were transfected with CDK1 siRNA for 72 h, followed by treatment with 20μM Nutlin in the last 24h. **A.** Microscopic images taken at 10x magnification before cells were harvested. **B.** Immunoblot analysis was performed to detect pHSF1, CDK1, CDK2, and p53. pHSF1 showed increased level in CDK1 depleted HCT116 cells. As a loading control, β-actin staining was performed.

RKO cells were also transfected with CDK1 siRNAs and treated with Nutlin as described for HCT116 cells in Figure 15. RKO cell density also decreased upon CDK1 knockdown (Fig. 16A). Immunoblot analysis represented an efficient siRNA transfection in RKO cells (Fig. 16B). Again, the expression level of pHSF1 increases in the CDK1-depleted RKO cells (Fig. 16B) as observed similarly in HCT116 cells (Fig. 15B).

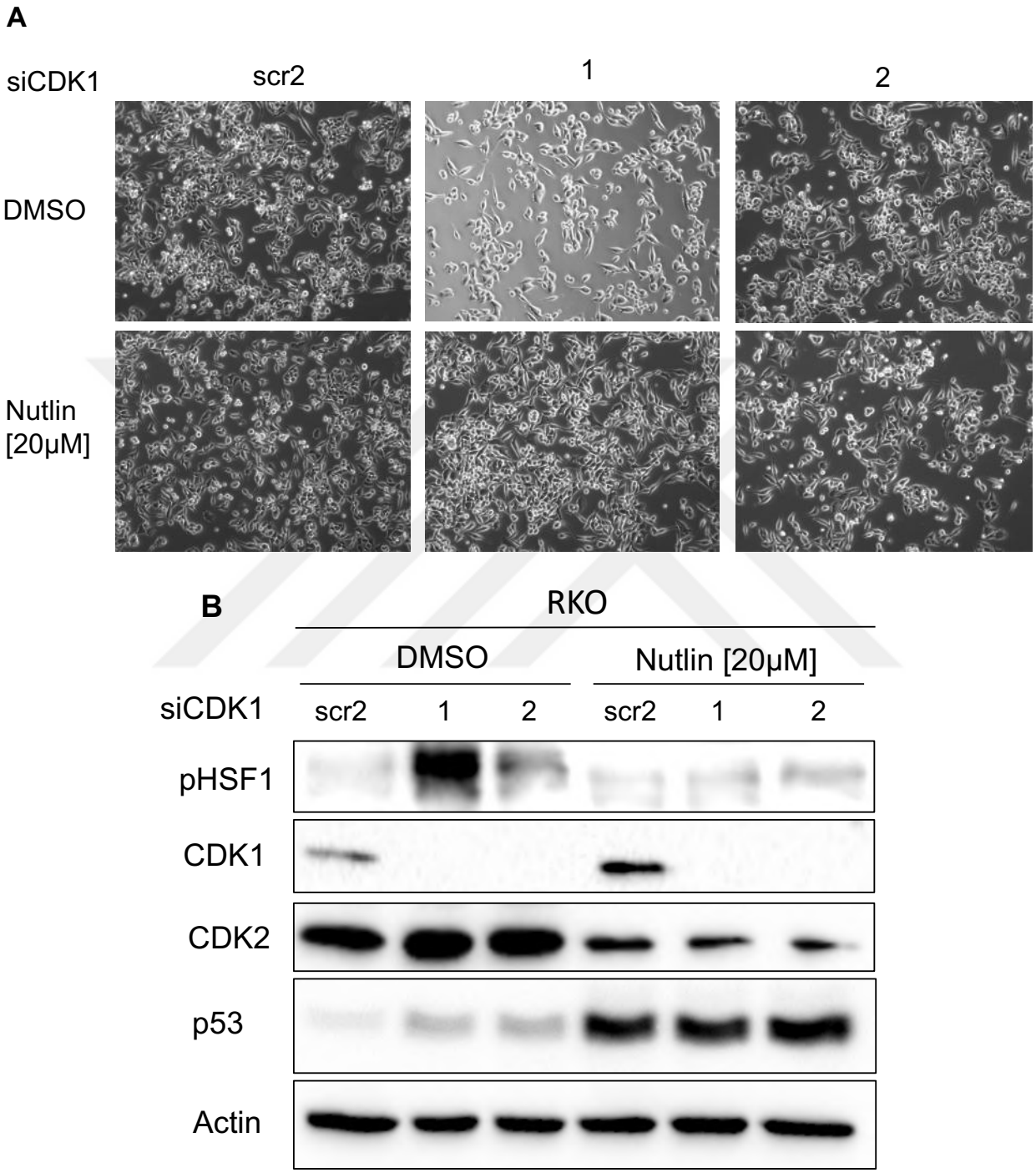

Figure 16: CDK1 depletion in RKO cells increases HSF1 phosphorylation. RKO cells were transfected with CDK1 siRNA for 72 h, followed by treatment with 20μM Nutlin in the last 24h. **A.** Microscopic images taken at 10x magnification before cells were harvested. **B.** Immunoblot analysis was performed to detect pHSF1, CDK1, CDK2 and p53. pHSF1 showed increased level in CDK1 depleted RKO cells. As a loading control, β-actin staining was performed.

CDK2 is repressed via p53 activation but CDK2 itself also mediates E2F activity (Fig. 4 in introduction) (Morris, Allen, & La Thangue, 2000). To analyse the regulatory effect of CDK2 on HSF1, HCT116 and RKO cells were transfected with CDK2 siRNAs (siCDK2-1 and siCDK2-2) for 72h and treated with Nutlin for final 24h. Cells were harvested to perform immunoblot analysis. As shown for CDK1, the HCT116 cell density is slightly decreased upon CDK2 knockdown cells compared to the controls (Fig. 17A). The cell density in RKO cells is not affected after siRNA transfection (Fig. 17C). In Figure 17B and D, the CDK2 staining represented that the knockdown was successful. Again, pHSF1 level increased in CDK2 depleted cells with and without Nutlin in HCT116 as well as RKO cells as seen in CDK1 depletion. Nutlin treatment alone reduced pHSF1 in both cell lines. In general, Nutlin treatment worked because the p53 level accumulated in treated cells compared to the controls.

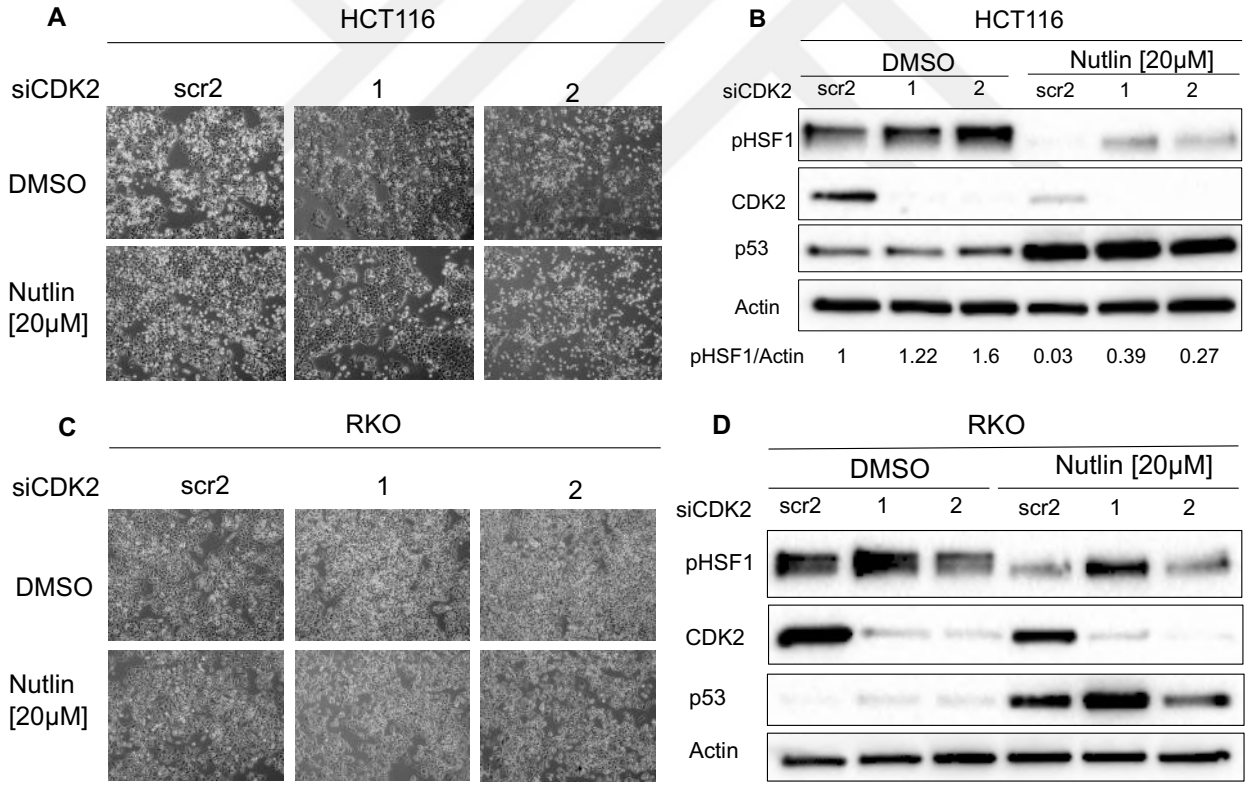

Figure 17: CDK2 depletion in HCT116 and RKO cells increases HSF1 phosphorylation. HCT116 cells were transfected with CDK2 siRNA for 72 h, followed by treatment with 20μM Nutlin in the last 24h. Microscopic images taken at 10x magnification before cells were harvested. **B.** Immunoblot analysis was performed to detect pHSF1, CDK2, p53 and β-actin. The ratio of quantification of pHSF1 to β-actin is just below of the blot. pHSF1 showed increased level in CDK2 depleted HCT116 cells. **C.** RKO cells were transfected with CDK2 siRNA for 72 h, followed by treatment with 20μM Nutlin in the last 24h. Microscopic images taken at 10x

magnification before cells were harvested. **D.** Immunoblot analysis was performed to detect pHSF1, CDK2, p53 and β-actin. pHSF1 showed increased level in CDK2 depleted RKO cells.

In summary, depletion of CDK1 or CDK2 increased phosphorylation of HSF1 on the contrary of our expectation. Thus, we withdraw the idea about CDKs in direct regulation of HSF1 activity. But importantly, depletion of both CDKs, CDK1 as well as CDK2, showed this upregulation of HSF1 activation pointing to reliable results although we cannot explain it yet.

4.3 Analysis of E2F-related target genes PLK4 and MLK3 for regulation of the HSF1 activity

Previous experiments showed that CDK1 and CDK2 kinase depletion increases HSF1 response which was an unexpected result. We thus tested other possible candidates; (I) the well-known E2F target PLK4 and (II) MLK3, not known to be an E2F target, but activates PLK4 in response to stress stimuli to protect cells from stress-induced apoptosis (Nakamura et al., 2013). qPCR results showed that mRNA level of PLK4 decreased in HCT116 cells after Nutlin treatment which confirms that PLK4 is an E2F target gene (Fig. 18A). MLK3 has not known yet as E2F target but MLK3 expression is partly rescued after Nutlin treatment in p53 depleted cells (Fig. 18B). Therefore, these two E2F-related genes which are dependent on p53, were selected to extend studies about HSF1 regulation.

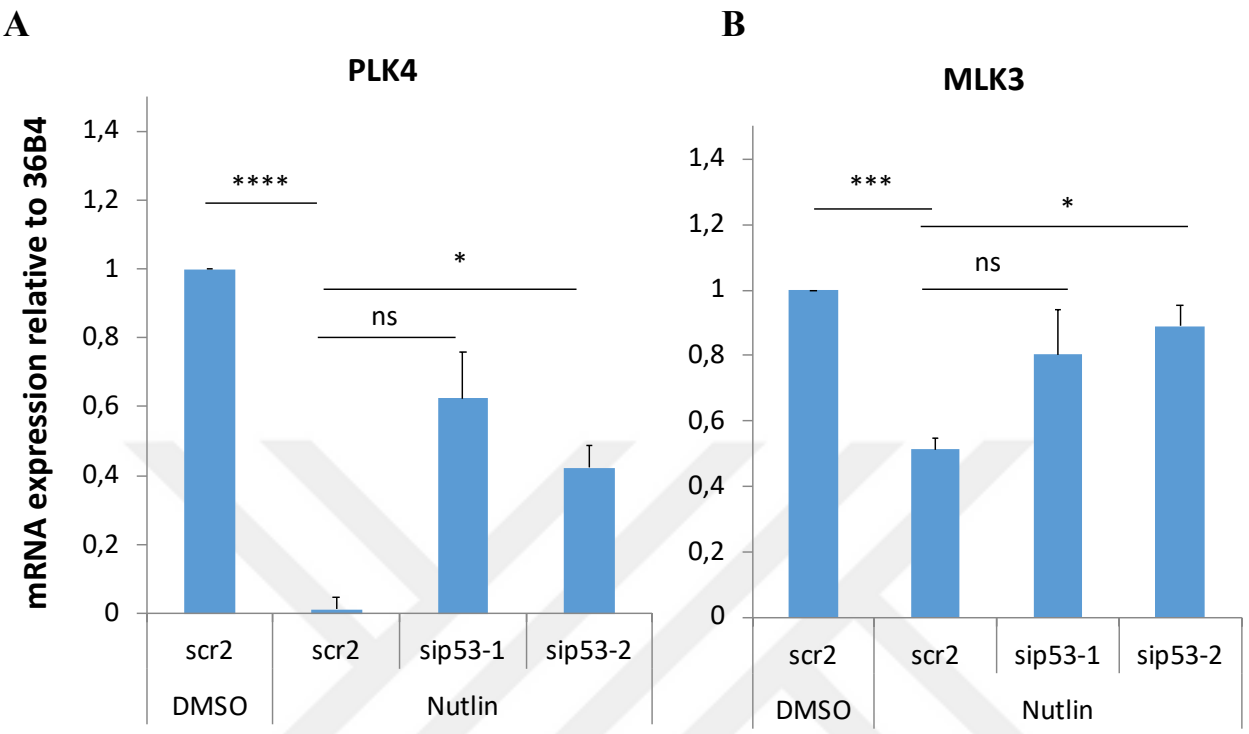

Figure 18: HCT116 cells depleted with p53 were analysed for the E2F-related target genes; PLK4 (A) and MLK3 (B). HCT116 cells were transfected with p53 siRNAs for 72h and treated with 20µl Nutlin for the final 24h. siRNA #2 that was treated with Nutlin displays a significant rescue effect for both PLK4 and MLK3 expression. qRT-PCR results as indicated were normalized to housekeeping gene 36B4 mRNA. Relative values are given in formula (2^{-ddCT}). Error bars indicate SEM of 2 independent experiments, repeated three times, each with all in duplicates. ns: non-significant, * P≤0.05, ** P≤0.01; *** P≤0.001; **** P≤0.0001.

4.4 PLK4, a possible candidate for HSF1 regulation

4.4.1 Inhibition of PLK4 by centrinone regulates HSF1 phosphorylation

In order to study the effect of PLK4 on HSF1 regulation, centrinone was used because it reversibly and selectively inhibits the activity of PLK4, which is active in centrosomes during centriole duplication. Different concentrations of centrinone treatment was tested in HCT116, RKO and LS174T cells for 48h. The cell density upon centrinone treatment decreased in HCT116 and RKO cells after 200nM compared to controls. With increasing centrinone concentrations (500nM-1µM)

the cell density remains the same as 200nM treated cells (Fig. 19A). HSF1 phosphorylation was analysed after centrinone treatment via immunoblot analysis.

Centrinone treatment decreased in PLK4 level compared to control in RKO cells (Fig. 19B). pHSF1 level was also decreased at 0.5 μM centrinone in RKO cells. Conversely, in HCT116 cells, PLK4 inhibition increased pHSF1 level. This is again an unexpected result since we expect if PLK4 is a HSF1 regulator, phosphorylation of HSF1 should decrease after PLK4 inhibition.

To elucidate whether PLK4 inhibition increases or decreases HSF1 phosphorylation, we decided to test a third wtp53-containing CRC cell line, LS174T.

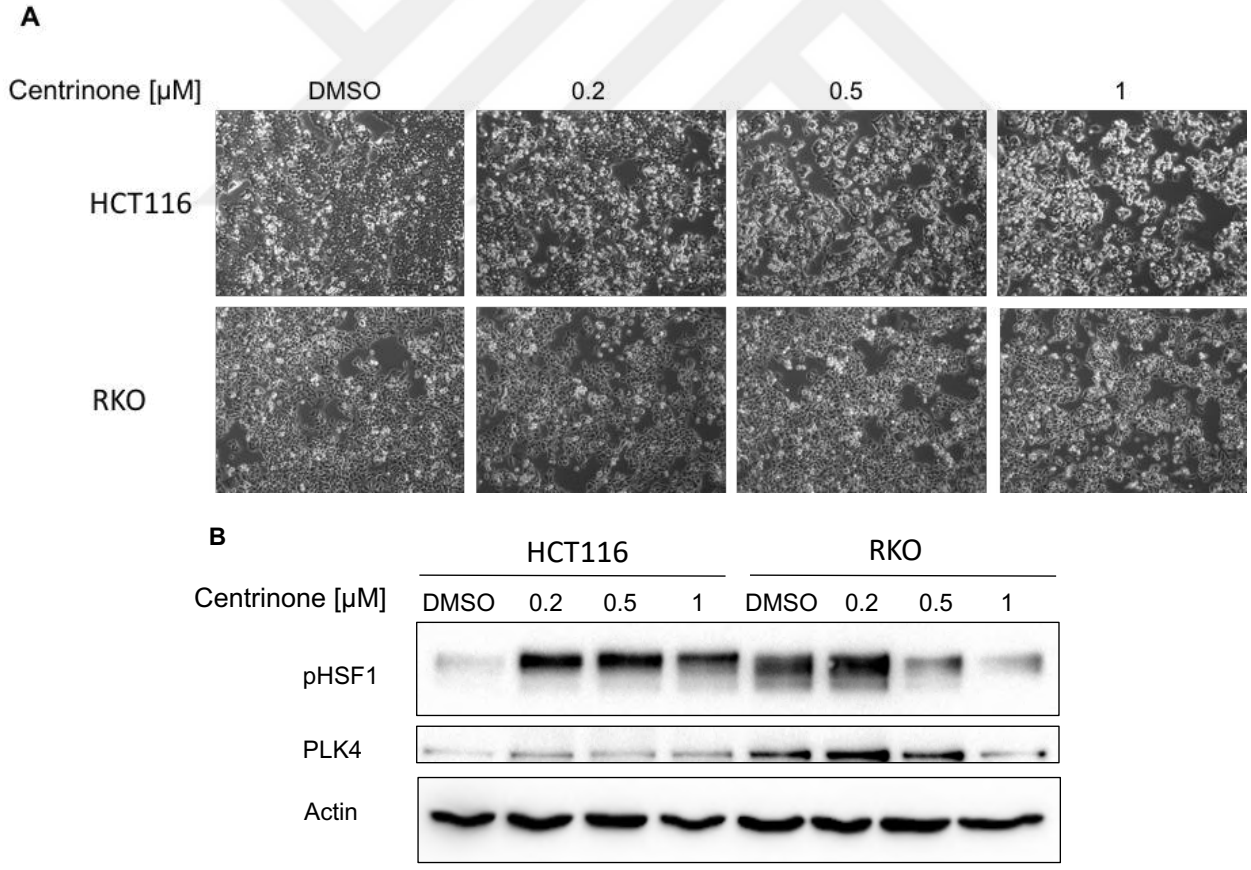

Figure 19: HCT116 and RKO cells treated with centrinone for 48h show slight decrease in HSF1 phosphorylation. A. HCT116 and RKO cells were treated with PLK4 inhibitor centrinone for 48h. Microscopic images taken at 10x magnification before cells were harvested. **B.** Immunoblot analysis was performed to detect pHSF1, PLK4 and β-actin. HCT116 cells treated

with centrinone showed increase on HSF1 level. Centrinone-treated RKO cells decreased HSF1 phosphorylation.

LS174T cells were treated with centrinone at different concentration (200-500-1000-2000nM) for 48h (Fig. 20). pHSF1 level decreased in centrinone-treated LS174T cells.

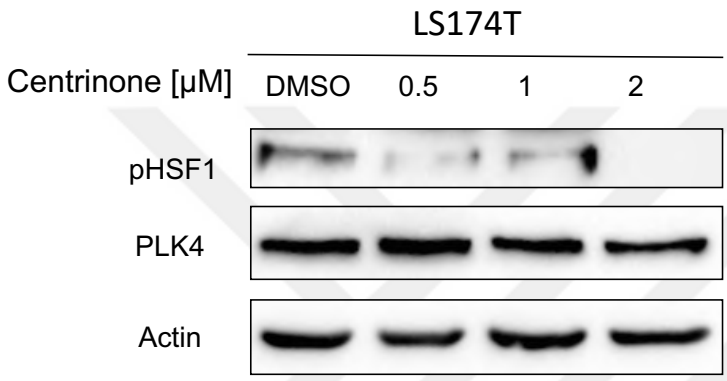

Figure 20: LS174T cells treated with centrinone for 48h show decrease in pHSF1 level.

LS174T cells were treated with PLK4 inhibitor namely centrinone for 48h. Cells were harvested and immunoblot analysis were performed for pHSF1 and PLK4. β-actin staining was performed as a loading control.

Since we detected the most effective response by centrinone in LS174T cells, we decided to analyse HSF1 response using LS174T cells (Fig. 21). After centrinone treatment (1 - 2µM) for 48h, RNA isolation was performed to analyse HSF1 target gene expression using HSP110 and RBBP5. PLK4 inhibition had no significant effect on HSP110 expression. However, PLK4 inhibition caused significant reduction in RBBP5 expression level compared to controls.

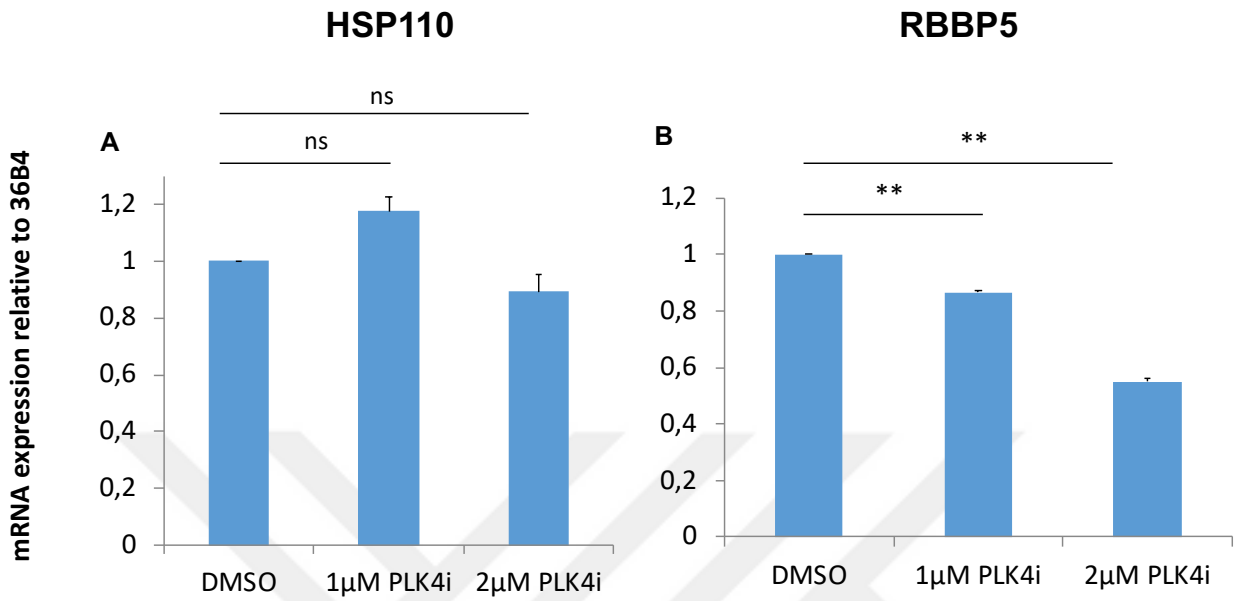

Figure 21: LS174T cells treated with centrinone for 48h show decrease expression of the HSF1 target RBBP5. LS174T cells were treated with 1 and 2µM PLK4 inhibitor centrinone for 48h. Cells were harvested, and qPCR analysis were performed for two of the HSF1 targets, HSP110 and RBBP5. Centrinone treated cells had significantly lower expression for RBBP5 but HSP110 expression had shown no significant change. qRT-PCR results as indicated were normalized to housekeeping gene 36B4 mRNA. Relative values are given in formula (2^{-ddCT}). Error bars indicate SEM of 2 independent experiments, repeated three times, each with all in duplicates. ns: non-significant, * P≤0.05, ** P≤0.01; *** P≤0.001; **** P≤0.0001.

4.4.2 Knock-down of PLK4 has no effective outcome in HSF1 protein level compared to HSF1 mRNA level

To further test the impact of PLK4 on HSF1, we decided to deplete total PLK4 protein level by siRNA. HCT116, RKO and LS174T cells were transfected with PLK4 targeted siRNAs for 72h and treated with Nutlin for final 24h. Surprisingly, immunoblot analysis showed no strong ablation of PLK4 protein after PLK4 silencing in untreated cells (DMSO) (Fig. 22). Only siPLK4-2 transfected HCT116 and RKO cells showed a slight decrease of PLK4 level (Fig. 22A-B). After Nutlin treatment, which led to strong decrease of PLK4 mRNA (Fig. 18A), PLK4 level after silencing were inconsistent. To exclude inefficiencies of our PLK4 siRNAs, we tested them on the level of mRNA. Therefore, we treated RKO cells as described above, isolated RNA to perform mRNA expression analysis of PLK4 (Fig. 23). And indeed, PLK4 mRNA was reduced after PLK4

silencing suggesting that PLK4 siRNAs worked. Importantly and in line, we know that Nutlin treatment leads to a strong decrease in PLK4 mRNA expression (Fig. 23). However, PLK4 protein level did not respond after Nutlin treatment. These observations lead to the hypothesis that PLK4 is a highly stabilized protein, although the literature is controversy regarding PLK4 stability (Holland et al., 2012; Holland, Lan, & Cleveland, 2010).

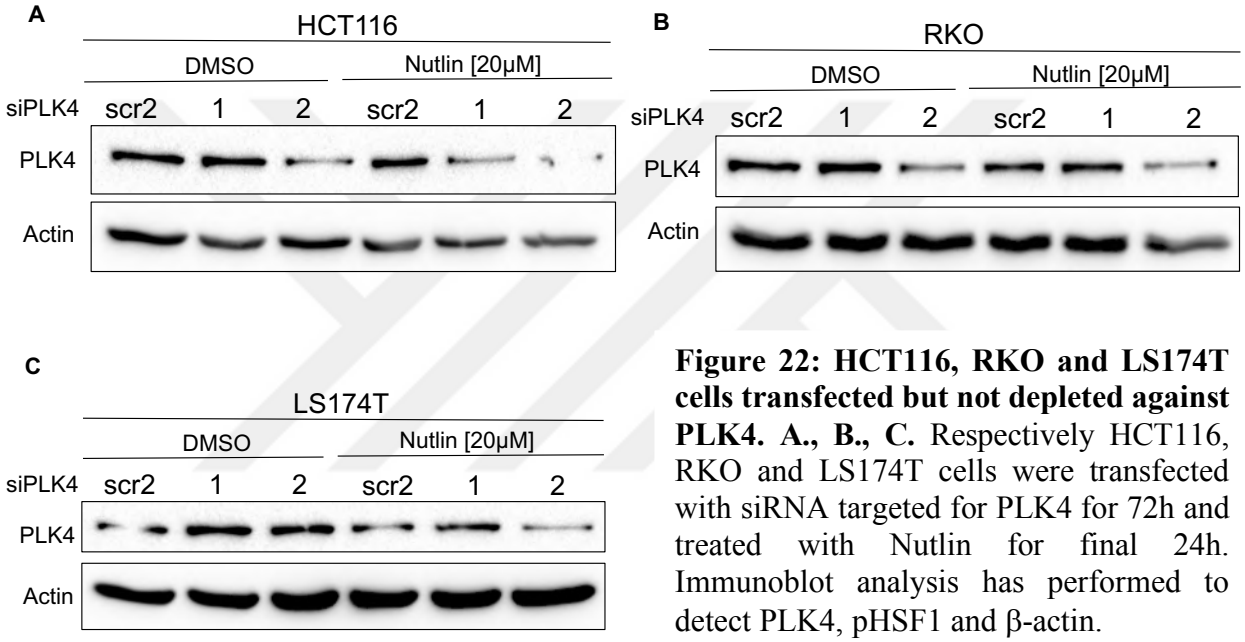

Figure 22: HCT116, RKO and LS174T cells transfected but not depleted against PLK4. A., B., C. Respectively HCT116, RKO and LS174T cells were transfected with siRNA targeted for PLK4 for 72h and treated with Nutlin for final 24h. Immunoblot analysis has performed to detect PLK4, pHSF1 and β-actin.

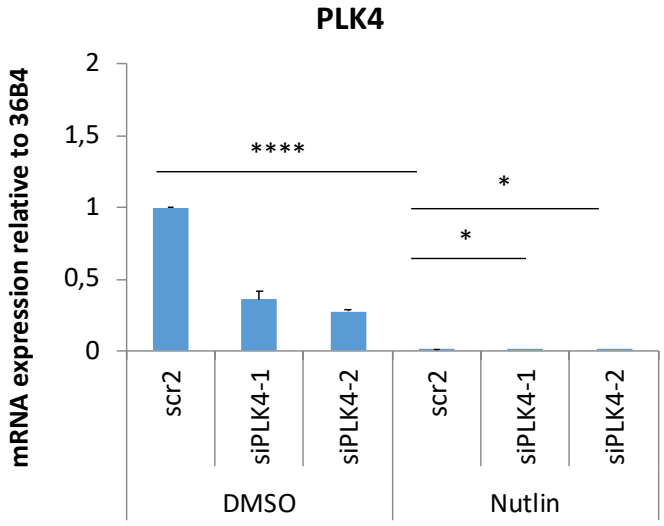

Figure 23: RKO cells transfected with siRNAs which are against to PLK4. RKO cells were transfected for 72h with siRNAs ad treated with Nutlin for last 24h. qRT-PCR results as indicated were normalized to housekeeping gene 36B4 mRNA. Relative values are given in formula (2^{-ddCT}). Error bars indicate SEM of 2 independent experiments, repeated twice, each with all in duplicates. ns: non-significant, * P≤0.05, ** P≤0.01; *** P≤0.001; **** P≤0.0001.

4.4.3 Identification of PLK4 as HSP90 client

To test how stable PLK4 protein is, we perform cycloheximide chase assays determining the half-life of PLK4. Cyclohexamide is an inhibitor of protein biosynthesis preventing the translational elongation. HCT116, RKO and LS174T cells treated with cycloheximide for 8 and 24h showed only slight reductions of PLK4 protein confirming our hypothesis that PLK4 is a stable protein (Fig. 24).

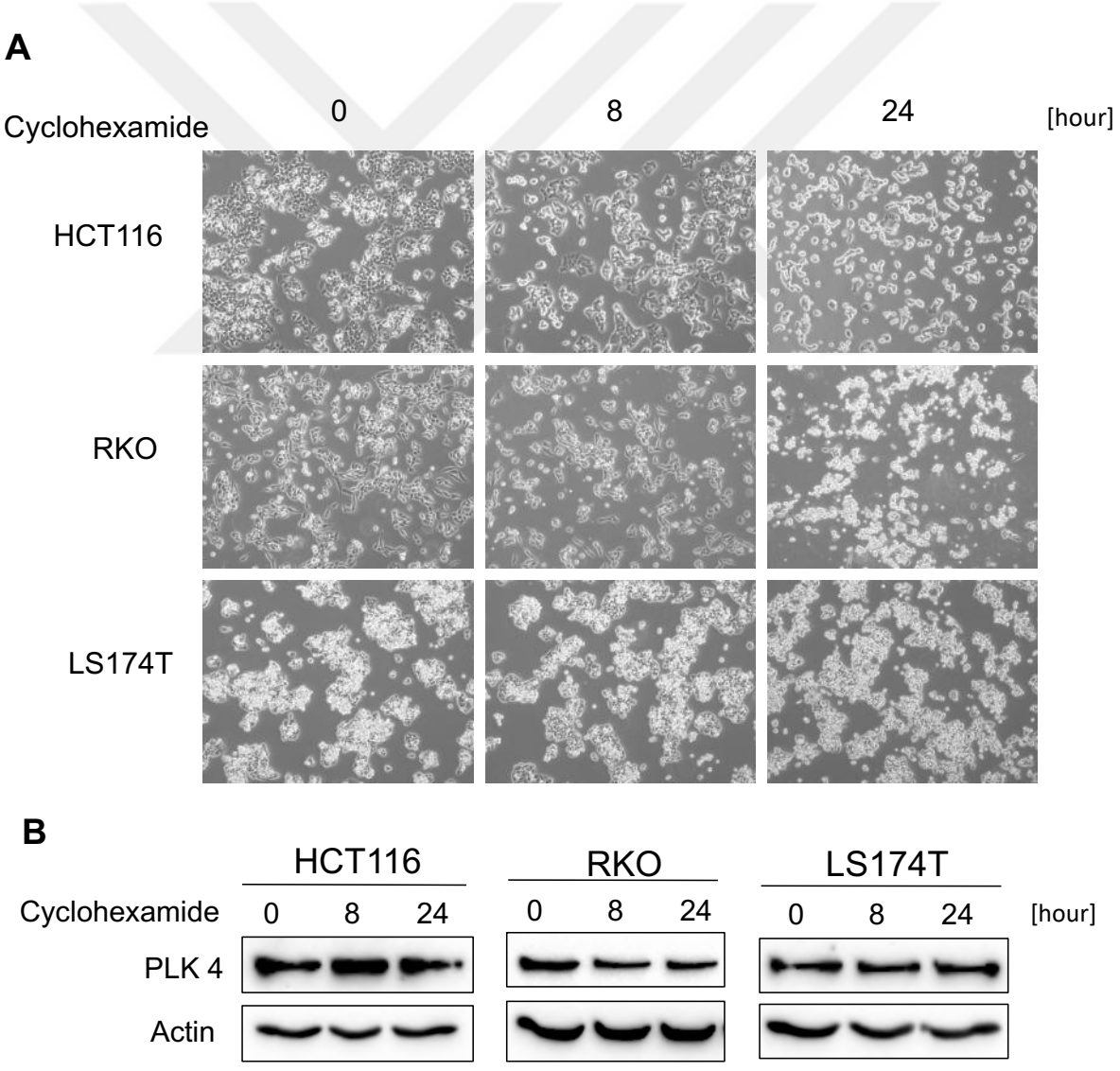

Figure 24: PLK4 is very stable protein since after 24h CHX treatment no reduction has been observed in HCT116, RKO and LS174T cells A. Microscopic images of HCT116, RKO and LS174T cells that were treated with CHX for 8 and 24h. Untreated cells have represented as controls. The microscopic images of HCT116, RKO and LS174T cells were taken at 10x

magnification after 0-8-24h periods of CHX treatment. Cell density has been reduced after 24h. **B.** Cells were harvested after CHX treatment and immunoblot analysis was performed to detect PLK4, and β-actin.

Since we identified that PLK4 is a stable protein, we asked whether this stabilization is mediated via the HSP90 system which is known to stabilize many oncogenic protein. Thus, we tested different HSP90 inhibitors which are geldanamycin, 17AAG and 17-DMAG in HCT116 and SW480 cells to block the activity of HSP90. HCT116 cells treated with geldanamycin and 17AAG showed a strong reduction of PLK4 level after 12h HSP90 inhibition (Fig. 25A). The increase size of pHSF1bands might point to ubiquitination of pHSF1 since it is known that HSP90 inhibition also induces degradation of HSF1itself. 17-DMAG treatment in HCT116 and SW480 cells was much stronger than the other inhibitors since the PLK4 level was completely vanished after 16h or 20h treatment (Fig. 25B). Thus, we identified that PLK4 as a new HSP90 client.

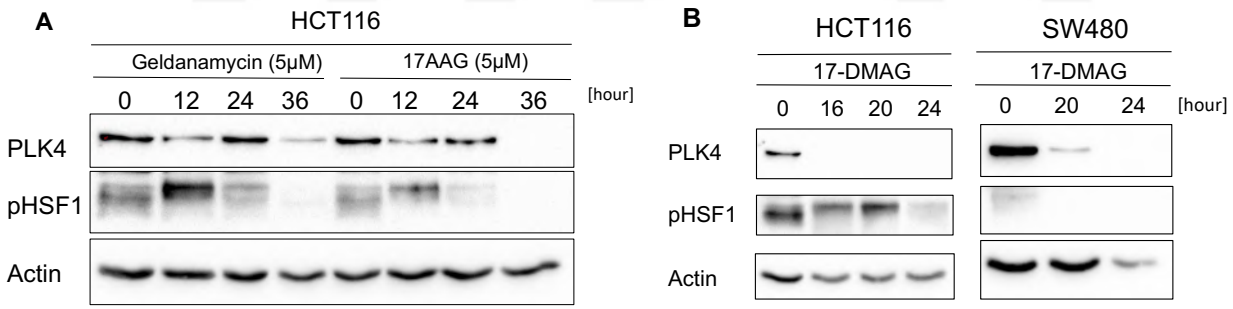

Figure 25: PLK4 protein level dramatically decreases after HSP90 inhibition in HCT116 and SW480 cells. A. HCT116 cells treated with HSP90 inhibitors; geldanamycin and 17-N-Allylamino-17-demethoxygeldanamycin (17AAG) which is semi-synthetic derivative of geldanamycin. 5 μM of geldanamycin and 17AAG were given to cells for 12-24 and 36h. Cells were harvested to perform immunoblot analysis for detecting PLK4, pHSF1 and β-actin. After 12h of treatment of both inhibitor causes PLK4 reduction. pHSF1 ubiquitinated through the treatment. **B.** 17-DMAG, another derivative of geldanamycin was given to the HCT116 and SW480 cells for 16-20 and 24h. After treatment cell were harvested and immunoblot analysis was done to detect PLK4, pHSF1 and β-actin. After 16h or 20h of 17-DMAG treatment, PLK4 level has been dramatically vanished and pHSF1 is ubiquitinated following by treatment hours.

After confirming PLK4 as HSP90-stabilized protein we were wondering when PLK4 protein disappears after Nutlin treatment. To answer this question, we performed long-term Nutlin treatment. HCT116, RKO and LS174T cells were treated for 5 or 10-day Nutlin. Nutlin treatment mediated a flat cell morphology and cell densities were greatly reduced compared to DMSO treated cells, because of the cell cycle arrest (Fig. 26). At day 10, cell densities were even less than the cells treated 5-day with Nutlin (Fig. 26). Following the cell harvesting, immunoblot detection was performed. RKO and LS174T cells showed a strong decrease of PLK4 protein at 5 and 10 days Nutlin (Fig. 27). Interestingly, HCT116 cells, which also did not respond after PLK4 inhibition via centrinone (Fig. 19B), also did not reduce PLK4 protein level after Nutlin long-term treatment (Fig. 27). However, pHSF1 bands shifted down after Nutlin long-term treatment pointing to a decrease in HSF1 modifications.

In summary, PLK4 is a possible candidate for HSF1 regulation although we can only show that RKO and LS174T cells respond after enzymatic PLK4 inhibition with centrinone. One major questionable point remains with the observation that PLK4 protein is stabilized via the HSP90 system. It is not well understood, whether PLK4 stability correlates with its enzymatic activity to regulate HSF1 or not. Normally, PLK4 is only active during S phase and stabilized PLK4 protein could serve as pool for rapid PLK4 activation. Thus, we do not know yet, whether Nutlin inhibits PLK4 kinase activity independently of down-regulation of PLK4 mRNA. It is not likely that p53-E2F regulates HSF1 via PLK4, just by down-regulation of PLK4 mRNA, but not PLK4 protein.

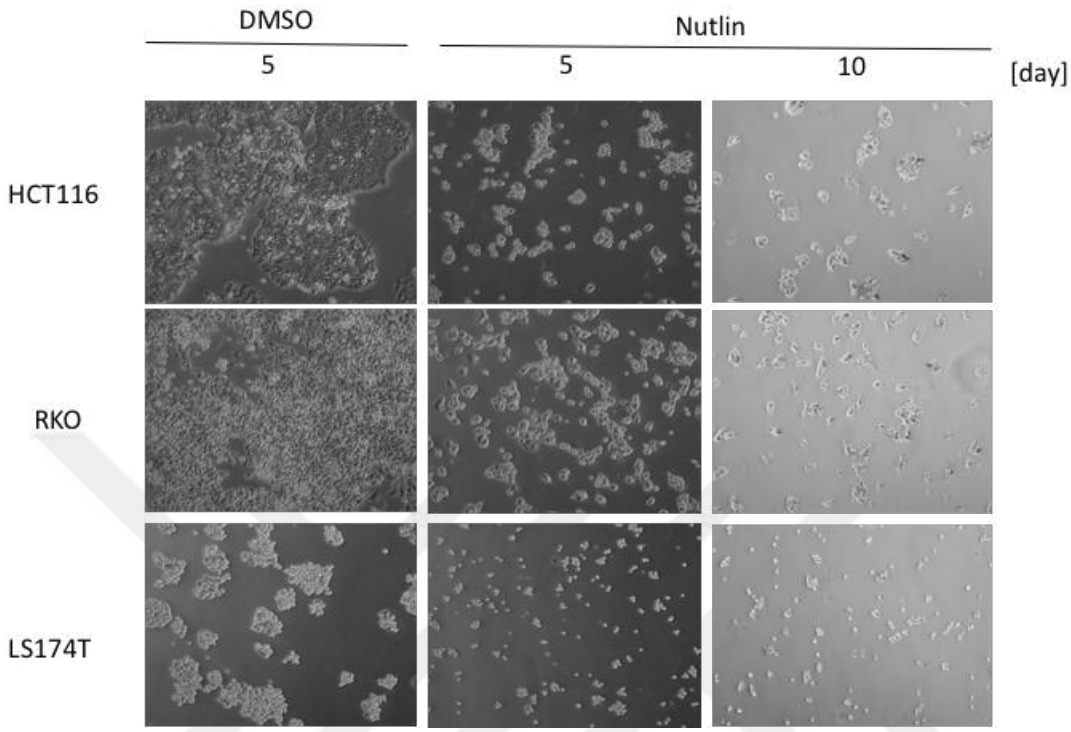

Figure 26: Microscopic images of HCT116, RKO and LS174T cells that were treated with DMSO and Nutlin for 5 and 10d. Cells that were treated with DMSO have represented the control group. The microscopic images of HCT116, RKO and LS174T cells were taken at 10x magnification after 5 and 10-day Nutlin treatment. Cell density was reduced after 5-day Nutlin treatment.

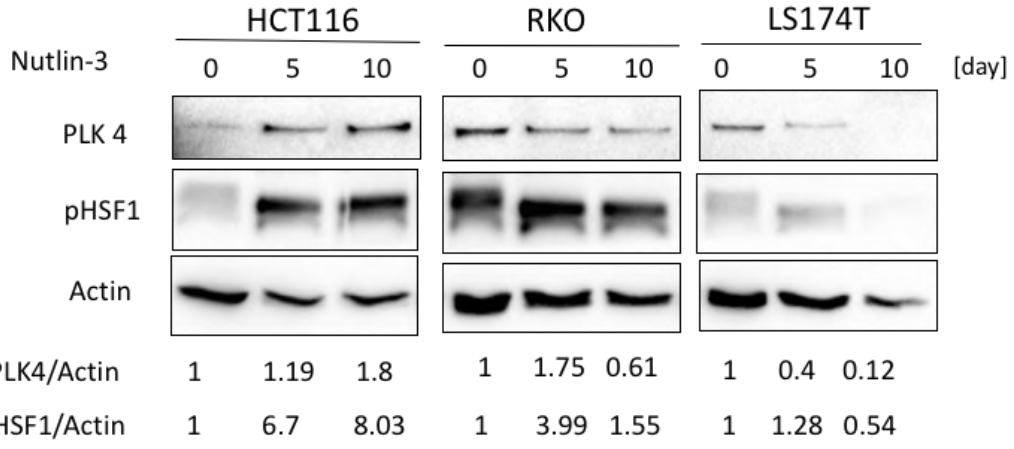

Figure 27: PLK4 is a stable protein; after 10-day Nutlin treatment, strong decrease was observed in RKO and LS174T cells but not in HCT116 cells. HCT116, RKO and LS174T cells were treated with Nutlin for 5 and 10-day to test the stability of PLK4. Cells were harvested and immunoblot analysis was performed to detect PLK4, pHSF1 and β-actin. The ratio of quantification of PLK4 and pHSf1 to β-actin is shown below of the blot.

4.5 MLK3, a strong candidate as HSF1 regulator

MLK3, a MAP3K, is connected to PLK4 as shown by Nakamura et al., 2013. During stress, prolonged PLK4 activity can lead to supernumerary chromosomes. PLK4 hyperactivity is cooperatively regulated by MAP3Ks-MAPK pathways involving p38 and JNK, and p53. Thus, p53 and MAP3K signalling cooperate to maintain centrosome integrity under stress conditions (Nakamura et al., 2013). As we identified MLK3 as E2F-regulated gene (Fig. 18B), we checked MLK3 as regulator of HSF1. HCT116 and RKO cells were transfected with MLK3 siRNAs (pool of three different siRNAs) for 72h and were treated with 20μM Nutlin for final 24h. Cell density was reduced after siMLK3 with and without Nutlin treatment (Fig. 28A).

Immunoblot analysis of these cells showed MLK3 depletion decreased PLK4 protein level as it was represented (Nakamura et al., 2013) (Fig. 28B). Importantly, knockdown of MLK3 alone already decreased pHSF1 in HCT116 cell as well as RKO cells, mimicking a p53-induced HSF1 repression by Nutlin alone.

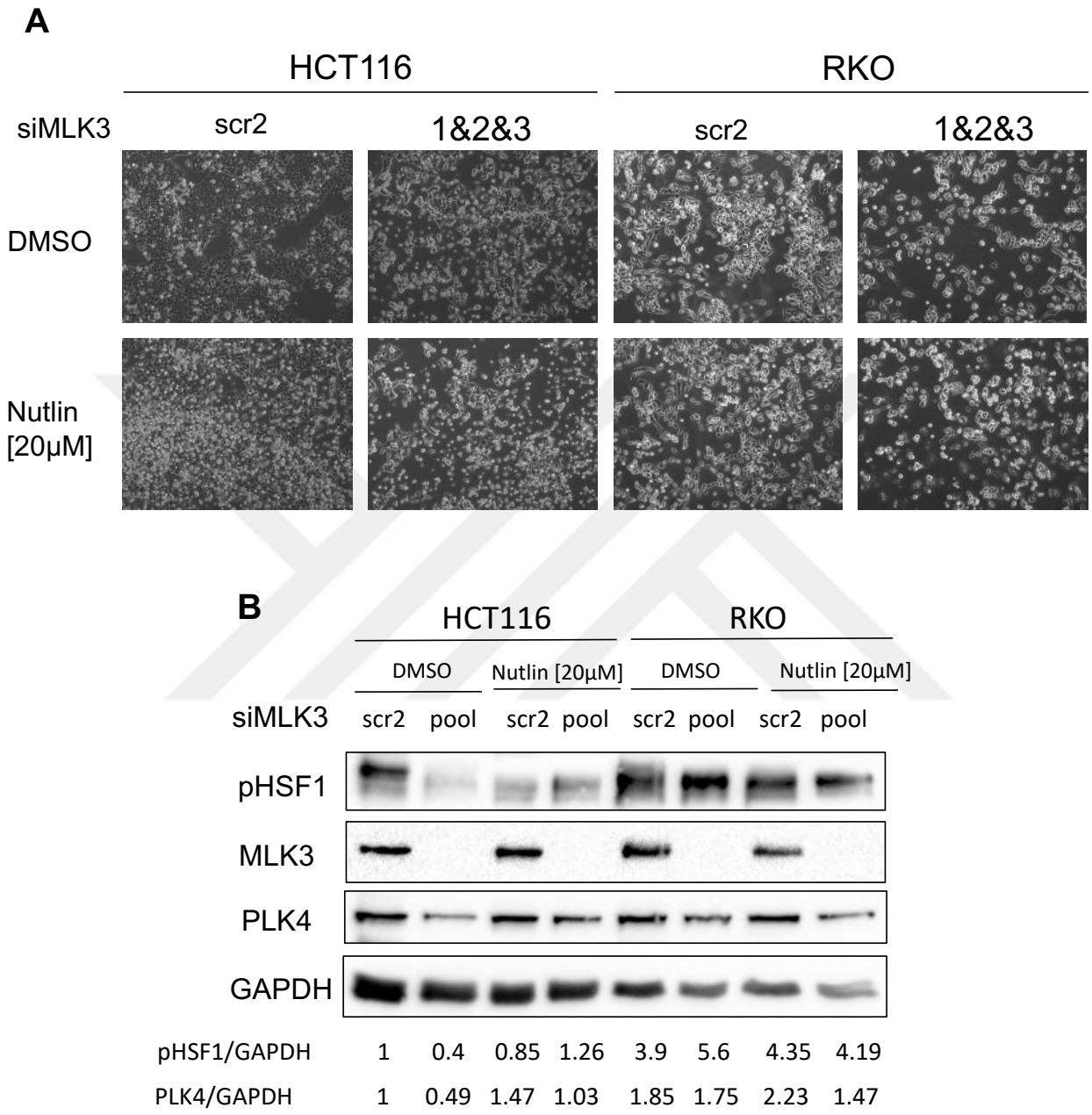

Figure 28: MLK3 depletion decreases pHSF1 in HCT116 and RKO cells. Both cell line was transfected with pooled of three different siRNA targeted to MLK3 for 72 h, followed by Nutlin treatment for final 24h. **A.** Microscopic images taken at 10x magnification. **B.** Immunoblot analysis was performed to detect pHSF1, MLK3, PLK4 and GAPDH. The ratio of quantification of pHSF1, PLK4 and to GAPDH is shown below of the blot.

Since the immunoblotting analysis show a clear decrease in HSF1 activity by decreased phosphorylation level of HSF1, we next checked the regulation of HSF1 target gene expression. HCT116 cells depleted for MLK3 have been tested for several HSF1 target genes which are HSP110, RBBP5, ITGB3BP and HSP90AA. HCT116 cells were transfected with MLK3 siRNAs (pool of three different siRNAs) for 72h and treated with 20µM Nutlin for final 24 h. Afterwards RNA was isolated to perform qPCR. MLK3 knockdown decreased significantly the expression of the HSF1 target genes tested (Fig. 29). Nutlin-treated HCT116 cells transfected with control siRNA confirmed our previous results of reduced HSP110, RBBP5, ITGB3BP and HSP90AA level after p53-induced HSF1 repression.

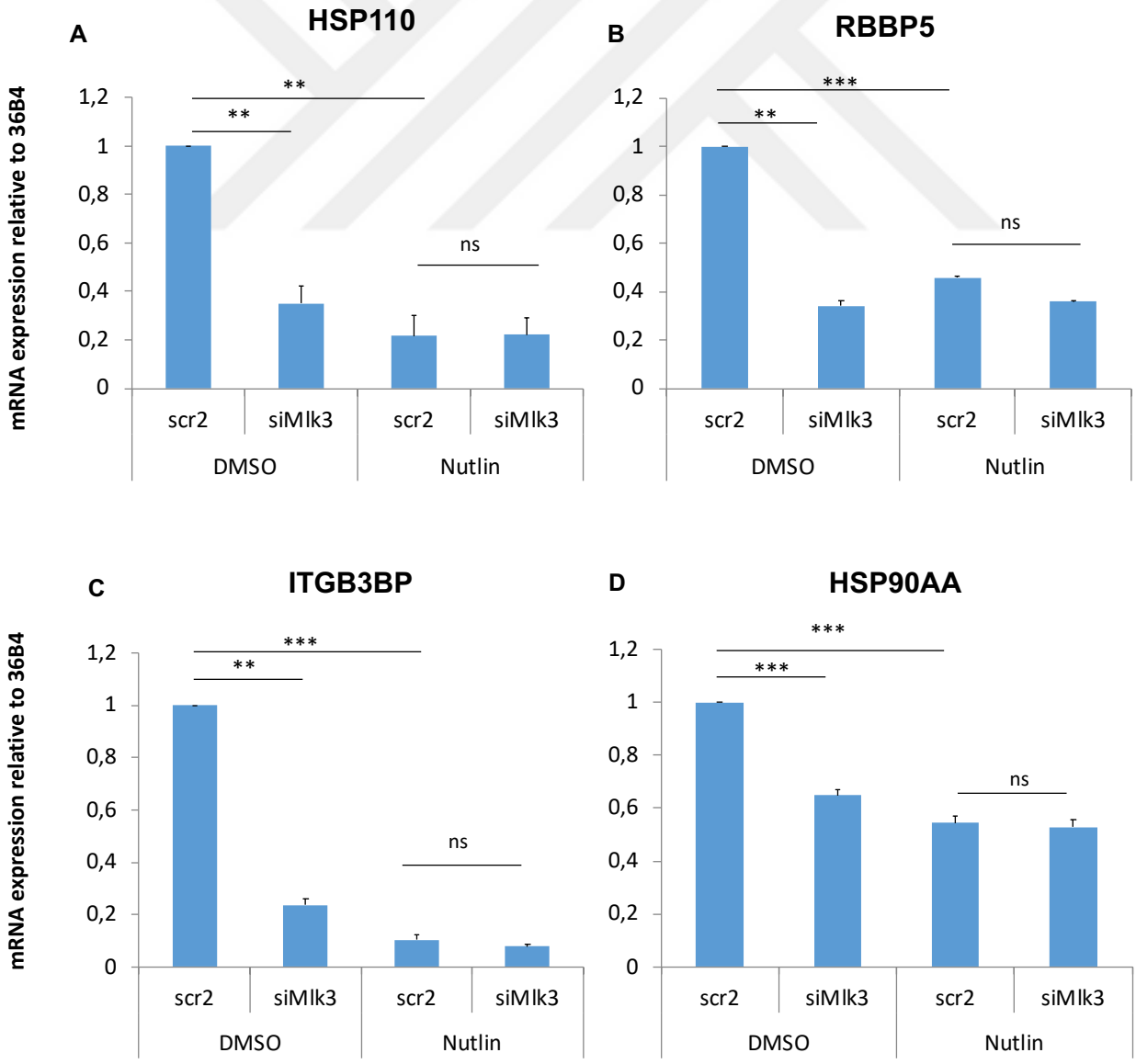

Figure 29: MLK3 depletion in HCT116 cells decreases expression of several HSF1 target genes. HCT116 cells were transfected with combined three different MLK3 siRNAs for 72h and treated with 20µl Nutlin for the last 24h. HCT116 cells that were depleted MLK3 have significant reduction in HSP110, RBP5, ITGB3BP and HSP90AA expression levels. qRT-PCR results as indicated were normalized to housekeeping gene 36B4 mRNA. Relative values are given in formula (2^{-ddCT}). Error bars indicate SEM of 2 independent experiments, repeated three times, each with all in duplicates. ns: non-significant, * P≤0.05, ** P≤0.01; *** P≤0.001; **** P≤0.0001.

4.6 MLK3 connects the p53-E2F response with the stress-induced MAPK kinases; MEK1/2

Previous studies demonstrated that MLK3 phosphorylates and activates MEK (Y. H. Shen et al., 2003) which itself regulates HSF1 (Ciocca et al., 2013). We identified that MLK3 is involved in HSF1 phosphorylation (Fig. 28). Thus, we tested whether the p53 regulates HSF1 via a direct MLK3-MEK1/2-HSF1 axis. First of all, we wanted to confirm the well-known p53 regulation on MEK stress pathway in our cell system (Singh, Upadhyay, Ajay, & Bhat, 2007). And indeed, immunoblot analysis performed in our CRC cell lines showed that p53 regulates MEK activity (Fig. 30).

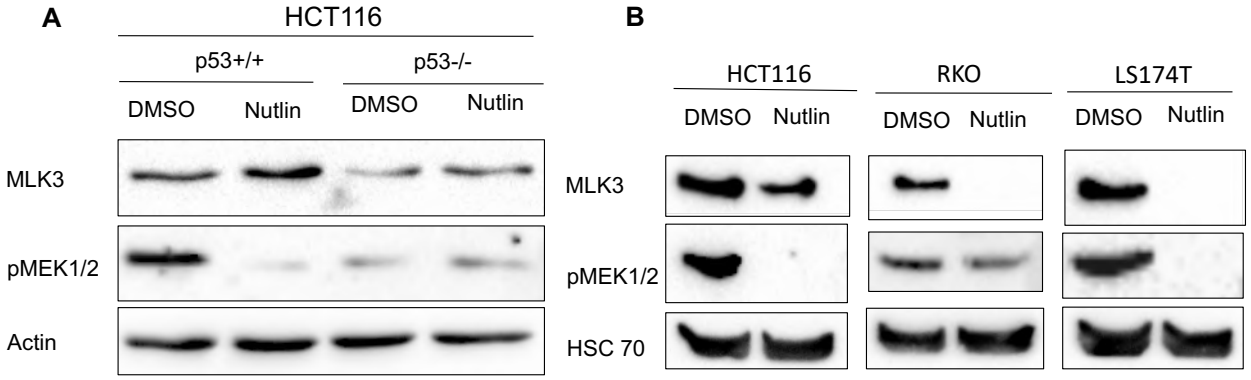

Figure 30: p53 regulates MEK activity. A. HCT116 with p53+/+ and p53 -/- cells treated by Nutlin. Immunoblot analysis was performed to detect MLK3, pMEK1/2 and β-actin as loading control. **B.** Immunoblot analysis was performed for HCT116, RKO and LS174T cells to detect MLK3, pMEK1/2 and HSC70 as loading control.

Next, we confirmed that MLK3 reduces pMEK1/2 activity (Fig. 31). Especially in HCT116 cells pMEK1/2 level were reduced upon MLK3 knockdown. The same effect was observed in RKO cells.

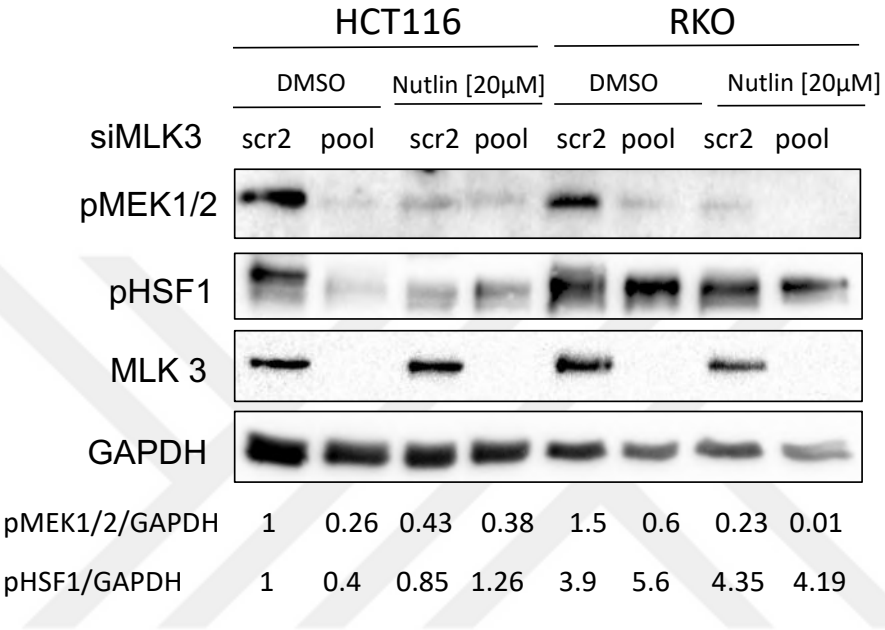

Figure 31: MLK3 depletion in HCT116 and RKO cells reduces pMEK1/2 activity. Both cell line was transfected with pool of three different siRNA targeted to MLK3 for 72 h, followed by Nutlin treatment for final 24h. Immunoblot analysis was performed to detect pMEK1/2, pHSF1, MLK3, and GAPDH. The ratio of quantification of pHSF1 and pMEK1/2 to GAPDH is shown below of the blot.

Interestingly our unexpected result from CDK1 knockdown (Fig. 15 and 16) can be explained with MEK1/2 activation. We observed a correlation between pMEK1/2 and pHSF1 (Fig. 32). After depletion of CDK1, MEK1/2 was activated as well as HSF1 was activated which might be a cell cycle stress response. MLK3 level also increases in CDK1 knockdown cells compared to controls (DMSO groups).

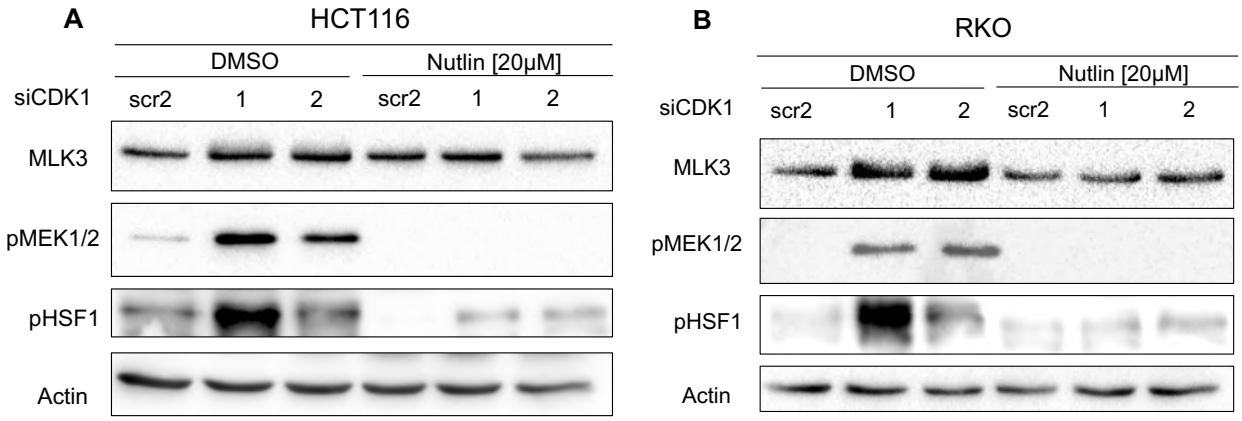

Figure 32: CDK1 depletion in HCT116 and RKO cells upregulates pMEK1/2 activity. Both cell lines were transfected with CDK1 siRNAs for 72 h, followed by Nutlin treatment for final 24h. Immunoblot analysis was performed to detect MLK3, pMEK1/2, pHSF1, and β-actin as loading control.

Another unexpected result was seen in HCT116 cells after PLK4 inhibition (Fig. 19B). Here HSF1 was increased after PLK4 inhibition, in huge contrast to RKO cells, where a PLK4 inhibition decreased pHSF1. And indeed, HCT116 we could detect an increase in pMEK1/2 which correlates with the increase of pHSF1 (Fig. 33), although we cannot explain yet why exclusively HCT116 respond with activation of stress pathways after PLK4 inhibition. In RKO cells, MEK phosphorylation did not respond to PLK4 inhibition. MLK3 level decreased upon inhibition of PLK4 in both cell lines.

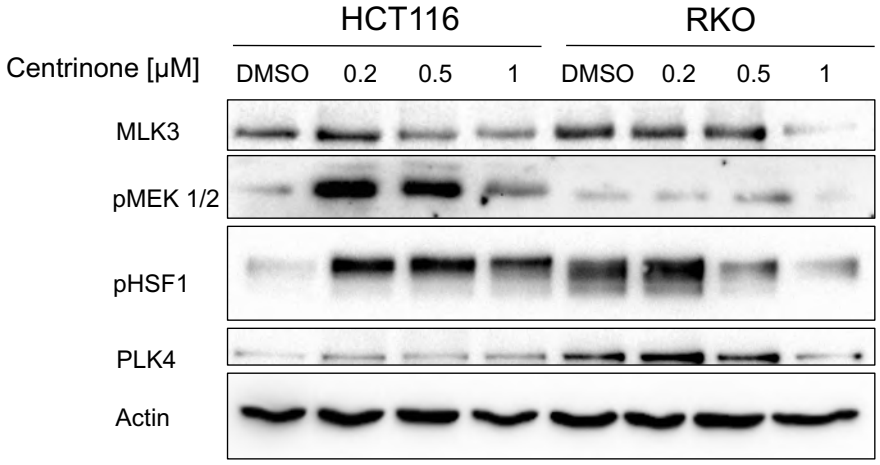

Figure 33: PLK4 inhibition upregulates pMEK1/2 activity in HCT116 cells in contrast to RKO cells. Both cell lines were treated for 48h, the treatment was refreshed in every 24h.

Immunoblot analysis was performed to detect MLK3, pMEK1/2, pHSF1, PLK4 and β-actin as loading control.

In conclusion, MLK3 is known to regulate MEK1/2 (Y. H. Shen et al., 2003) and MEK1/2 is known to regulate HSF1 (Tang et al., 2015). We clarified now that a linear signalling pathway exists via MLK3-MEK1/2-HSF1 in colorectal cancer cells.

5. Discussion

The tumor suppressor p53 has several roles such as cell cycle arrest, apoptosis or DNA repair to protect the cell from damage (Kaiser & Attardi, 2017). Thereby, p53 activates a wide range of target genes to suppress tumorigenesis and importantly among these target genes, p21 regulates the CDKs (Agarwal et al., 1995). In response to damage, p21 inhibits CDKs and prevent entry to S phase since E2F target gene expression has been blocked. p53-E2F related genes are able to manage cellular stress to maintain cell integrity. So far, our hypothesis was that wtp53 regulates HSF1-HSP90 system via E2F-related genes such as CDK1, CDK2, PLK4 and MLK3. To test this hypothesis, the phosphorylation level of HSF1 as well as its target gene expressions were analysed in Nutlin activated wtp53 CRC cell lines. Our study identified that p53-mediated E2F repression leads to decrease in MLK3 expression which subsequently reduces the MEK1/2-mediated HSF1 phosphorylation.

According to the results, we showed that MLK3 is a connection between the cell cycle and stress pathways.

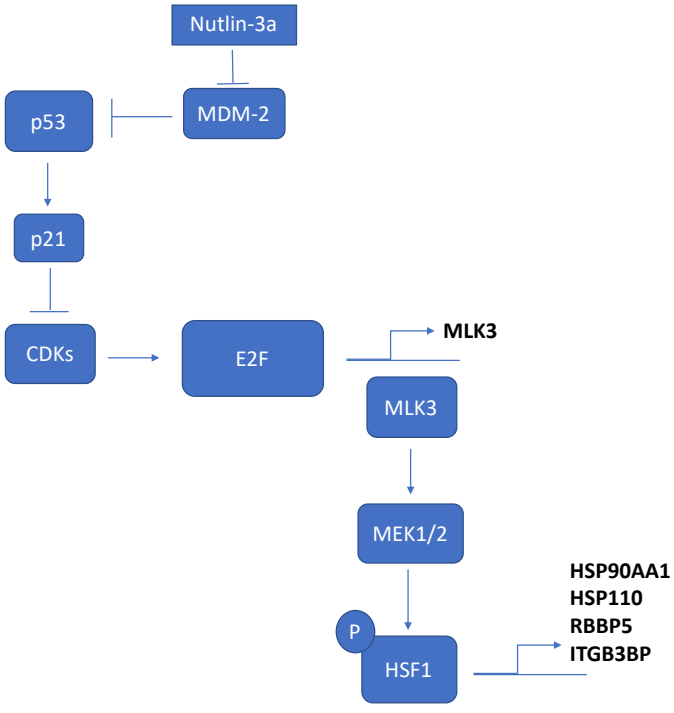

Figure 34: A hypothetical cartoon demonstrates the relation between MLK3 and HSF1 regulation.

Although we identified that MLK3 activates HSF1, whether this is the main route is still unclear. The network of p53 and stress pathways are quite diverse and complicated, and we cannot exclude other axes in other cell systems.

Regarding on HSF1-Ser326 regulation, the main route seems to involve MEK1/2, a well-known enzyme which physically interacts and phosphorylates HSF1 at Ser326 residue (Guettouche, Boellmann, Lane, & Voellmy, 2005). HSF1 undergoes a series of phosphorylation events, among which Ser326 phosphorylation stimulates its activation. Importantly, MEK is regulated via several pathways within the cellular and cell cycle-related stress response. In our study, we investigated in p53-E2F-related genes; CDK1, PLK4 and MLK3 which might modify HSF1-Ser326 phosphorylation. This does not exclude other cell cycle-regulated genes which were not addressed in our studies.

5.1 CDK1 depletion increases HSF1 phosphorylation

The immunoblot experiments with siRNA depletion of CDK1 gave the insight that pMEK1/2 and MLK3 is upregulated in HCT116 and RKO cells. Correlated with increase in MEK1 activity, HSF1 phosphorylation increases as well (Fig 32). Many studies have shown that CDK1 is the rate limiting factor for the G2 to M transition and CDK1 level was diminished significantly in HSF1-/- and 17AAG treated oocytes (Kanatsu-Shinohara, Schultz, & Kopf, 2000; Metchat et al., 2009). Although we expected a decrease in HSF1 activity after CDK1 depletion if CDK1 would directly regulate HSF1 activity, we observed an increase of HSF1 phosphorylation. In this case, CDK1 depletion induced stress in cells and that might increase in pMEK1/2 and subsequently HSF1 activation. Studies have shown that pMEK1/2 level increases during G2 to M transition (Feinstein & Linstedt, 2006) and that targeting CDK1 and MEK/ERK overcomes cell death and resistance (P. Zhang et al., 2018). MEK1 is in general known as meiosis and mitosis associate kinase (Hollingsworth, 2016). Thus, CDK1 knockdown induced MEK1/2 activation which leads subsequently to HSF1 activation.

As an E2F-related gene within the cell cycle, CDK2 was tested as well. Cells with CDK2 knockdown also increased HSF1 phosphorylation similarly as CDK1 depletion. Unfortunately

staining for pMEK1/2 and MLK3 are not done yet to correlate CDK2 depletion to stress-activated MEK1/2.

5.2 PLK4 inhibition has different outcomes in different cell lines

Another E2F-related gene PLK4 was also tested to understand the mechanism behind HSF1 regulation. PLK4 was inhibited by using centrinone in HCT116, RKO and LS174T cells. HCT116 cells differentially responded than RKO and LS174T cells upon PLK4 inhibition. HSF1 phosphorylation was increased after PLK4 inhibition in HCT116 cells and again MEK activity was increased as similarly HSF1 does. On the other hand, in RKO cells, PLK4 inhibition did not induce stress since MEK activity remains same which correlates with pHSF1 stability. The reason why there is a very special route in stress response in HCT116 cells than RKO and LS174T cells remains elusive. One possible explanation might be because of the mutations that HCT116 cells harbor; CDKN2A, CTNNB1(B-catenin), PIK3CA and kRAS but there is no supportive literature found related with stress pathway.

The centrinone treatment performed at different concentrations (0.2-0.5-1-2μM) did not show effective changes in PLK4 level in all tested cell lines (Fig. 19 and 20) which leads to arise a question about PLK4 stability. However, PLK4 stability is controversial in the literature. In normal cells, PLK4 abundance is tightly regulated in order to correctly control centrosome number and maintain genome integrity (Holland et al., 2010). It is a low-abundance kinase whose stability is directly linked to its autophosphorylation. It has demonstrated that autoregulated instability controls the abundance of endogenous PLK4. Preventing PLK4 autoregulation leads to centrosome amplification and p53 stabilization. Therefore, self-catalyzed destruction of endogenous PLK4 plays a critical role in suppressing PLK4 protein level to limit centriole duplication to the production of one new centrosome per cell cycle (Holland et al., 2012).

In mammalian cells, stress stimuli activate specific intracellular signaling network that dictates a cell fate ranging from cell survival to apoptosis (Nakamura et al., 2013). PLK4 can be phosphorylated by different MAP3K in response to specific stress factors. Additionally, prolonged stress conditions trigger the activation of tumor suppressor p53 which downregulates PLK4 expression to promote apoptosis and therefore preventing centrosome amplification. Thus, PLK4

expression was strongly repressed by wild-type p53 in several human tumor cell models (Maniswami et al., 2018). Importantly, in our situation we observed that PLK4 is a stable protein in wt-p53 containing cancer cell lines (Fig. 18, 22-24).

At the end of analyzing PLK4 stability, we identified that PLK4 as a HSP90 client. The HSP90 is well-known as protective system for diverse tumor-prone proteins and oncogenes. One paper has already suggested PLK4 as client but within a screen among lots other kinases and without further validation (A. Haupt et al., 2012). We validated and confirmed that in several cell lines; HCT116 and SW480 and using different HSP90 inhibitors; geldanamycin, 17 AAG and DMAG (Fig. 25).

Additionally, we determined that long-term Nutlin treatment vanished at the end PLK4 protein in RKO and LS174T cells. But again, HCT116 cells differed with their response and increased PLK4 level was observed instead of decrease. Important to know is that stabilized PLK4 might not mean that Plk4 is always active as enzyme. From the literature we know that PLK4 mRNA expression was low during quiescent, G0 and early-to-mid G1 phase in mouse fibroblasts (Maniswami et al., 2018). The expression increases through S phase and peaks during S, G2 and M phases (Fode, Binkert, & Dennis, 1996). PLK4 becomes active only during S phase with the activity almost doubled during G2 phases (Sillibourne & Bornens, 2010). Maybe stabilized PLK4 serves as pool for rapid PLK4 activation.

It could also easily be that stabilized Plk4 cannot perform enzymatic activity anymore or can gain new enzymatic-independent functions. Unfortunately, there is no available sufficient antibody against an active PLK4 modification site. Unfortunately, antibodies against well-accepted PLK4 substrates did not work in our hands. PLK4 kinase activity assays could be a possibility and might be performed for further analysis. In conclusion, we are not able to determine yet whether stable PLK4 protein is also enzymatically active after p53 activation via Nutlin.

5.3 MLK3 depletion decrease HSF1 activity via MEK pathway

Importantly and in line with the previous finding that MEK1 regulates HSF1, also our unexpected results can be explained by stress-induced MEK activation. We identified MLK3 as a p53-E2F-

regulated gene, and MLK3 is known to regulate MEK. Thus, we assume that the MLK3-MEK axis is an important route for p53-mediated HSF1 regulation.

We tested HCT116 cells which seem to be very sensitive to stress, with MLK3 siRNA. Unfortunately, we could not test RKO and LS174T cells with MLK3 siRNA because of time limitations. MLK3-depleted HCT116 cells showed that MLK3 regulates HSF1 phosphorylation (Fig. 28). MLK3 depletion in HCT116 cells also decreases HSF1 target gene expression dramatically in mRNA level (Fig. 29) which strongly refers to MLK3 as an important component of stress-meditated HSF1 regulation. It is shown that MLK3 is chaperoned by HSP90 and overexpressed in malignant cells (Chen, Miller, & Gallo, 2010; H. Zhang et al., 2004). Our finding corresponds to the literature, so we further investigated the role of MEK in MLK3 triggered HSF1 pathway. Cross talk between JNK/SAPK and ERK/MAPK rather than a linear cascade has already shown. Additionally, it is reported that MLK3 activates MEK1/2 in vitro and induces MEK phosphorylation at its activation sites in vivo (Y. H. Shen et al., 2003). Therefore, what we observed as seen in figure 28 and 31, knocking-down MLK3 decreases MEK as well as HSF1 phosphorylation dramatically in HCT116 and RKO cells.

5.4 Conclusion and future perspectives

Our findings present that p53 represses HSF1 activity via MLK3-MEK1/2 axis in tumor cells with a homozygous p53 situation. Such repression of the HSF1 system, as a major tumor-driving system, might enforce a selective pressure to alter wtp53 function through e.g. TP53 mutations. Given that tumors which are heterozygous for wtp53, still have residual p53 transcription capacity, it would be important to analyse whether p53 heterozygous tumors are also able to repress the HSF1 activity. Such selective force might be going to inactivate the remaining wtp53 allele. This hypothesis is only testable in *in vivo* CRC mouse models since it does not exist a human CRC cell line with such genetic background.

Further, we identified that one of the E2F-related gene, PLK4, is a stable protein as it is HSP90 client. Unfortunately, its regulatory effect on HSF1 is still an open question. However, the identification of PLK4 as HSP90 clients opens the question whether tumor cells rely on PLK4

independent of its enzymatic kinase function, since it seems to be well-accepted that PLK4 is only active during S phase.

6. References

Agarwal, M. L., Agarwal, A., Taylor, W. R., & Stark, G. R. (1995). p53 controls both the G2/M and the G1 cell cycle checkpoints and mediates reversible growth arrest in human fibroblasts. *Proceedings of the National Academy of Sciences of the United States of America*, *92*(18), 8493–8497. https://doi.org/10.1073/pnas.92.18.8493

Aksoy, O., Chicas, A., Zeng, T., Zhao, Z., McCurrach, M., Wang, X., & Lowe, S. W. (2012). The atypical E2F family member E2F7 couples the p53 and RB pathways during cellular senescence. *Genes and Development*, *26*(14), 1546–1557. https://doi.org/10.1101/gad.196238.112

Alexandrova, E. M., Mirza, S. A., Xu, S., Schulz-Heddergott, R., Marchenko, N. D., & Moll, U. M. (2017). P53 loss-of-heterozygosity is a necessary prerequisite for mutant p53 stabilization and gain-of-function in vivo. *Cell Death and Disease*, *8*(3). https://doi.org/10.1038/cddis.2017.80

Alexandrova, E. M., Yallowitz, A. R., Li, D., Xu, S., Schulz, R., Proia, D. A., … Moll, U. M. (2015). Improving survival by exploiting tumour dependence on stabilized mutant p53 for treatment. *Nature*, *523*(7560), 352–356. https://doi.org/10.1038/nature14430

Anckar, J., & Sistonen, L. (2007). Heat shock factor 1 as a coordinator of stress and developmental pathways. *Advances in Experimental Medicine and Biology*. https://doi.org/10.1007/978-0-387-39975-1_8

Archambault, V., & Glover, D. M. (2009). Polo-like kinases: Conservation and divergence in their functions and regulation. *Nature Reviews Molecular Cell Biology*. https://doi.org/10.1038/nrm2653

Benson, E. K., Mungamuri, S. K., Attie, O., Kracikova, M., Sachidanandam, R., Manfredi, J. J., & Aaronson, S. A. (2014). P53-dependent gene repression through p21 is mediated by recruitment of E2F4 repression complexes. *Oncogene*, *33*(30), 3959–3969. https://doi.org/10.1038/onc.2013.378

Bertoli, C., Skotheim, J. M., & De Bruin, R. A. M. (2013). Control of cell cycle transcription during G1 and S phases. *Nature Reviews Molecular Cell Biology*. https://doi.org/10.1038/nrm3629

Bettencourt-Dias, M., Rodrigues-Martins, A., Carpenter, L., Riparbelli, M., Lehmann, L., Gatt, M. K., … Glover, D. M. (2005). SAK/PLK4 is required for centriole duplication and flagella development. *Current Biology*, *15*(24), 2199–2207. https://doi.org/10.1016/j.cub.2005.11.042

Bieging, K. T., Mello, S. S., & Attardi, L. D. (2014). Unravelling mechanisms of p53-mediated tumour suppression. *Nature Reviews Cancer*. https://doi.org/10.1038/nrc3711

Bio-Rad. (2018). What is Real-Time PCR (qPCR)? Retrieved from http://www.bio-rad.com/de-de/applications-technologies/what-real-time-pcr-qpcr?ID=LUSO4W8UU

Brosh, R., & Rotter, V. (2009). When mutants gain new powers: News from the mutant p53 field. *Nature Reviews Cancer*. https://doi.org/10.1038/nrc2693

Calvisi, D. F., Simile, M. M., Ladu, S., Frau, M., Evert, M., Tomasi, M. L., … Pascale, R. M. (2011). Activation of v-Myb avian myeloblastosis viral oncogene homolog-like2 (MYBL2)-LIN9 complex contributes to human hepatocarcinogenesis and identifies a subset of hepatocellular carcinoma with mutant p53. *Hepatology*, *53*(4), 1226–1236. https://doi.org/10.1002/hep.24174

Carvajal, L. A., Hamard, P. J., Tonnessen, C., & Manfredi, J. J. (2012). E2F7, a novel target, is up-regulated by p53 and mediates DNA damage-dependent transcriptional repression. *Genes and Development*, *26*(14), 1533–1545. https://doi.org/10.1101/gad.184911.111

Chen, J., Miller, E. M., & Gallo, K. A. (2010). MLK3 is critical for breast cancer cell migration and promotes a malignant phenotype in mammary epithelial cells. *Oncogene*, *29*(31), 4399–4411. https://doi.org/10.1038/onc.2010.198

Chesnoy, S., & Huang, L. (2000). Structure and Function of Lipid-DNA Complexes for Gene Delivery. *Annual Review of Biophysics and Biomolecular Structure*, *29*(1), 27–47. https://doi.org/10.1146/annurev.biophys.29.1.27

Ciocca, D. R., Arrigo, A. P., & Calderwood, S. K. (2013). Heat shock proteins and heat shock factor 1 in carcinogenesis and tumor development: An update. *Archives of Toxicology*. https://doi.org/10.1007/s00204-012-0918-z

Dimitriadi, M., Poulogiannis, G., Liu, L., Bäcklund, L. M., Pearson, D. M., Ichimura, K., & Collins, V. P. (2008). p53-independent mechanisms regulate the P2-MDM2 promoter in adult astrocytic tumours. *British Journal of Cancer*, *99*(7), 1144–1152. https://doi.org/10.1038/sj.bjc.6604643

El-Deiry, W. S., Kern, S. E., Pietenpol, J. A., Kinzler, K. W., & Vogelstein, B. (1992). Definition of a consensus binding site for p53. *Nature Genetics*, *1*(1), 45–49. https://doi.org/10.1038/ng0492-45

el-Deiry, W. S., Tokino, T., Velculescu, V. E., Levy, D. B., Parsons, R., Trent, J. M., … Vogelstein, B. (1993). WAF1, a potential mediator of p53 tumor suppression. *Cell*, *75*(4), 817–825. https://doi.org/10.1016/0092-8674(93)90500-P

Elsevier B.V. (2012). Reverse transcription polymerase chain reaction. Retrieved from https://www.sciencedirect.com/topics/neuroscience/reverse-transcription-polymerase-chain-reaction

Feinstein, T. N., & Linstedt, A. D. (2006). Mitogen-activated Protein Kinase Kinase 1-dependent Golgi Unlinking Occurs in G2 Phase and Promotes the G2/M Cell Cycle Transition. *Molecular Biology of the Cell*, *18*(2), 594–604. https://doi.org/10.1091/mbc.E06-06-0530

Ferlay, J., Soerjomataram, I., Dikshit, R., Eser, S., Mathers, C., Rebelo, M., … Bray, F. (2015). Cancer incidence and mortality worldwide: Sources, methods and major patterns in GLOBOCAN 2012. *International Journal of Cancer*, *136*(5), E359–E386. https://doi.org/10.1002/ijc.29210

Fischer, M. (2017). Census and evaluation of p53 target genes. *Oncogene*. https://doi.org/10.1038/onc.2016.502

Fischer, M., Grossmann, P., Padi, M., & DeCaprio, J. A. (2016). Integration of TP53, DREAM, MMB-FOXM1 and RB-E2F target gene analyses identifies cell cycle gene regulatory

networks. *Nucleic Acids Research*, *44*(13), 6070–6086. https://doi.org/10.1093/nar/gkw523

Fischer, M., Quaas, M., Nickel, A., & Engeland, K. (2015). Indirect p53-dependent transcriptional repression of <i>Survivin, CDC25C,</i> and <i>PLK1</i> genes requires the cyclin-dependent kinase inhibitor p21/CDKN1A and CDE/CHR promoter sites binding the DREAM complex. *Oncotarget*, *6*(39), 41402–41417. https://doi.org/10.18632/oncotarget.6356

Fischer, M., Quaas, M., Steiner, L., & Engeland, K. (2016). The p53-p21-DREAM-CDE/CHR pathway regulates G2/M cell cycle genes. *Nucleic Acids Research*, *44*(1), 164–174. https://doi.org/10.1093/nar/gkv927

Fode, C., Binkert, C., & Dennis, J. W. (1996). Constitutive expression of murine Sak-a suppresses cell growth and induces multinucleation. *Molecular and Cellular Biology*, *16*(9), 4665–4672.

Freed-Pastor, W. A., & Prives, C. (2012). Mutant p53: One name, many proteins. *Genes and Development*, *26*(12), 1268–1286. https://doi.org/10.1101/gad.190678.112

Funk, W. D., Pak, D. T., Karas, R. H., Wright, W. E., & Shay, J. W. (1992). A transcriptionally active DNA-binding site for human p53 protein complexes. *Molecular and Cellular Biology*, *12*(6), 2866–2871. https://doi.org/10.1128/MCB.12.6.2866.Updated

George, A., & Urch, C. (2000). *Diagnostic and Therapeutic Antibodies. Methods in Molecular Medicine*. Humana Press.

Guettouche, T., Boellmann, F., Lane, W. S., & Voellmy, R. (2005). Analysis of phosphorylation of human heat shock factor 1 in cells experiencing a stress. *BMC Biochemistry*, *6*. https://doi.org/10.1186/1471-2091-6-4

Habedanck, R., Stierhof, Y. D., Wilkinson, C. J., & Nigg, E. A. (2005). The Polo kinase Plk4 functions in centriole duplication. *Nature Cell Biology*, *7*(11), 1140–1146. https://doi.org/10.1038/ncb1320

Haupt, A., Joberty, G., Bantscheff, M., Fröhlich, H., Stehr, H., Schweiger, M. R., … Lange, B. M. H. (2012). Hsp90 inhibition differentially destabilises MAP kinase and TGF-beta signalling

components in cancer cells revealed by kinase-targeted chemoproteomics. *BMC Cancer*, *12*. https://doi.org/10.1186/1471-2407-12-38

Haupt, Y., Maya, R., Kazaz, A., & Oren, M. (1997). Mdm2 promotes the rapid degradation of p53. *Nature*, *387*(6630), 296–299. https://doi.org/10.1038/387296a0

Hirko, A., Tang, F., & Hughes, J. A. (2003). Cationic lipid vectors for plasmid DNA delivery. *Current Medicinal Chemistry*, *10*(14), 1185–1193. https://doi.org/10.2174/0929867033457412

Holland, A. J., Fachinetti, D., Zhu, Q., Bauer, M., Verma, I. M., Nigg, E. A., & Cleveland, D. W. (2012). The autoregulated instability of Polo-like kinase 4 limits centrosome duplication to once per cell cycle. *Genes and Development*, *26*(24), 2684–2689. https://doi.org/10.1101/gad.207027.112

Holland, A. J., Lan, W., & Cleveland, D. W. (2010). Centriole duplication: A lesson in self-control. *Cell Cycle*. https://doi.org/10.4161/cc.9.14.12184

Hollingsworth, N. M. (2016). Mek1/Mre4 is a master regulator of meiotic recombination in budding yeast. *Microbial Cell*, *3*(3), 129–131. https://doi.org/10.15698/mic2016.03.487

International Agency for Research on Cancer. (2008). World Cancer report 2008. *Cancer Control*, *199*, 512. https://doi.org/10.1016/j.cma.2010.02.010

Invitrogen by Life. (2013). Lipofectamine® 2000 Reagent.

Joerger, A. C., & Fersht, A. R. (2010). The tumor suppressor p53: from structures to drug discovery. *Cold Spring Harbor Perspectives in Biology*. https://doi.org/10.1101/cshperspect.a000919

Kaiser, A. M., & Attardi, L. D. (2017). Deconstructing networks of p53-mediated tumor suppression in vivo. *Cell Death and Differentiation*. https://doi.org/10.1038/cdd.2017.171

Kanatsu-Shinohara, M., Schultz, R. M., & Kopf, G. S. (2000). Acquisition of Meiotic Competence in Mouse Oocytes: Absolute Amounts of p34cdc2, Cyclin B1, cdc25C, and wee1 in

Meiotically Incompetent and Competent Oocytes1. *Biology of Reproduction*, *63*(6), 1610–1616. https://doi.org/10.1095/biolreprod63.6.1610

Kastan, M. B., Onyekwere, O., Sidransky, D., Vogelstein, B., & Craig, R. W. (1991). Participation of p53 protein in the cellular response to DNA damage. *Cancer Research*, *51*(23 Pt 1), 6304–6311.

Kojima, K., Konopleva, M., McQueen, T., O'Brien, S., Plunkett, W., & Andreeff, M. (2006). Mdm2 inhibitor Nutlin-3a induces p53-mediated apoptosis by transcription-dependent and transcription-independent mechanisms and may overcome Atm-mediated resistance to fludarabine in chronic lymphocytic leukemia. *Blood*, *108*(3), 993–1000.

Koo, L. C., Mang, O. W., & Ho, J. H. (1997). An ecological study of trends in cancer incidence and dietary changes in Hong Kong. *Nutrition and Cancer*, *28*(3), 289–301. https://doi.org/10.1080/01635589709514590

Krempels, D. M. (n.d.). The Genetics of Cancer Regulation of cell number and division. Retrieved May 24, 2018, from http://www.bio.miami.edu/dana/250/250S12_15print.html

Kruse, J. P., & Gu, W. (2009). Modes of p53 Regulation. *Cell*. https://doi.org/10.1016/j.cell.2009.04.050

Levine, A. J., & Oren, M. (2009). The first 30 years of p53: Growing ever more complex. *Nature Reviews Cancer*. https://doi.org/10.1038/nrc2723

Lin, D., Shields, M. T., Ullrich, S. J., Appella, E., & Mercer, W. E. (1992). Growth arrest induced by wild-type p53 protein blocks cells prior to or near the restriction point in late G1 phase. *Proceedings of the National Academy of Sciences of the United States of America*, *89*(19), 9210–9214. https://doi.org/10.1073/pnas.89.19.9210

Litovchick, L., Sadasivam, S., Florens, L., Zhu, X., Swanson, S. K., Velmurugan, S., … DeCaprio, J. A. (2007). Evolutionarily Conserved Multisubunit RBL2/p130 and E2F4 Protein Complex Represses Human Cell Cycle-Dependent Genes in Quiescence. *Molecular Cell*, *26*(4), 539–551. https://doi.org/10.1016/j.molcel.2007.04.015

Liu, Z., Sekito, T., Špiírek, M., Thornton, J., & Butow, R. A. (2003). Retrograde signaling is regulated by the dynamic interaction between Rtg2p and Mks1p. *Molecular Cell*, *12*(2), 401–411. https://doi.org/10.1016/S1097-2765(03)00285-5

Maniswami, R. R., Prashanth, S., Karanth, A. V., Koushik, S., Govindaraj, H., Mullangi, R., … Jegatheesan, S. K. (2018). PLK4: a link between centriole biogenesis and cancer. *Expert Opinion on Therapeutic Targets*. https://doi.org/10.1080/14728222.2018.1410140

Mendrysa, S. M., & Perry, M. E. (2000). The p53 tumor suppressor protein does not regulate expression of its own inhibitor, MDM2, except under conditions of stress. *Molecular and Cellular Biology*, *20*(6), 2023–2030. https://doi.org/10.1128/MCB.20.6.2023-2030.2000

Metchat, A., Akerfelt, M., Bierkamp, C., Delsinne, V., Sistonen, L., Alexandre, H., & Christians, E. S. (2009). Mammalian heat shock factor 1 is essential for oocyte meiosis and directly regulates Hsp90α expression. *Journal of Biological Chemistry*, *284*(14), 9521–9528. https://doi.org/10.1074/jbc.M808819200

Mihara, M., Erster, S., Zaika, A., Petrenko, O., Chittenden, T., Pancoska, P., & Moll, U. M. (2003). p53 has a direct apoptogenic role at the mitochondria. *Molecular Cell*, *11*(3), 577–590. https://doi.org/10.1016/S1097-2765(03)00050-9

Moll, U. M., & Petrenko, O. (2003). The MDM2-p53 interaction. *Molecular Cancer Research : MCR*, *1*(14), 1001–1008. https://doi.org/10.1016/s0092-8674(00)81871-1

Morris, L., Allen, K. E., & La Thangue, N. B. (2000). Regulation of E2F transcription by cyclinE-Cdk2 kinase mediated through p300/CBP co-activators. *Nature Cell Biology*, *2*(4), 232–239. https://doi.org/10.1038/35008660

Müller, G. A., Stangner, K., Schmitt, T., Wintsche, A., & Engeland, K. (2016). Timing of transcription during the cell cycle: Protein complexes binding to E2F, E2F/CLE, CDE/CHR, or CHR promoter elements define early and late cell cycle gene expression. *Oncotarget*, *26*(4), 7–8. https://doi.org/10.18632/oncotarget.10888

Nakamura, T., Saito, H., & Takekawa, M. (2013). SAPK pathways and p53 cooperatively regulate PLK4 activity and centrosome integrity under stress. *Nature Communications*, *4*.

https://doi.org/10.1038/ncomms2752

Neidler, S. (2017). What are the differences between PCR, RT-PCR, qPCR, and RT-qPCR? Retrieved from http://www.enzolifesciences.com/science-center/technotes/2017/march/what-are-the-differences-between-pcr-rt-pcr-qpcr-and-rt-qpcr

Parikh, N., Hilsenbeck, S., Creighton, C. J., Dayaram, T., Shuck, R., Shinbrot, E., … Donehower, L. A. (2014). Effects of TP53 mutational status on gene expression patterns across 10 human cancer types. *Journal of Pathology*, *232*(5), 522–533. https://doi.org/10.1002/path.4321

Petitjean, A., Mathe, E., Kato, S., Ishioka, C., Tavtigian, S. V., Hainaut, P., & Olivier, M. (2007). Impact of mutant p53 functional properties on TP53 mutation patterns and tumor phenotype: Lessons from recent developments in the IARC TP53 database. *Human Mutation*, *28*(6), 622–629. https://doi.org/10.1002/humu.20495

Prives, C., & Hall, P. A. (1999). The P53 pathway. *Journal of Pathology*. https://doi.org/10.1002/(SICI)1096-9896(199901)187:1<112::AID-PATH250>3.0.CO;2-3

Quaas, M., Müller, G. A., & Engeland, K. (2012). p53 can repress transcription of cell cycle genes through a p21WAF1/CIP1-dependent switch from MMB to DREAM protein complex binding at CHR promoter elements. *Cell Cycle*, *11*(24), 4661–4672. https://doi.org/10.4161/cc.22917

Riley, T., Sontag, E., Chen, P., & Levine, A. (2008). Transcriptional control of human p53-regulated genes. *Nature Reviews Molecular Cell Biology*, *9*(5), 402–412. https://doi.org/10.1038/nrm2395

Roxburgh, P., Hock, A. K., Dickens, M. P., Mezna, M., Fischer, P. M., & Vousden, K. H. (2012). Small molecules that bind the Mdm2 RING stabilize and activate p53. *Carcinogenesis*, *33*(4), 791–798. https://doi.org/10.1093/carcin/bgs092

Sadasivam, S., & DeCaprio, J. A. (2013). The DREAM complex: Master coordinator of cell cycle-dependent gene expression. *Nature Reviews Cancer*. https://doi.org/10.1038/nrc3556

Sarge, K. D., Murphy, S. P., & Morimoto, R. I. (1993). Activation of heat shock gene transcription by heat shock factor 1 involves oligomerization, acquisition of DNA-binding activity, and

nuclear localization and can occur in the absence of stress. *Molecular and Cellular Biology*, *13*(3), 1392–1407. https://doi.org/10.3109/02656739609027676

Schmit, F., Korenjak, M., Mannefeld, M., Schmitt, K., Franke, C., Von Eyss, B., … Gaubatz, S. (2007). LINC, a human complex that is related to pRB-containing complexes in invertebrates regulates the expression of G2/M genes. *Cell Cycle*, *6*(15), 1903–1913. https://doi.org/10.4161/cc.6.15.4512

Shapiro, A. L., Viñuela, E., & V. Maizel Jr., J. (1967). Molecular weight estimation of polypeptide chains by electrophoresis in SDS-polyacrylamide gels. *Biochemical and Biophysical Research Communications*, *28*(5), 815–820. https://doi.org/10.1016/0006-291X(67)90391-9

Shen, H., & Maki, C. G. (2011). Pharmacologic activation of p53 by small-molecule MDM2 antagonists. *Curr Pharm Des*, *17*(6), 560–568. https://doi.org/10.2174/138161211795222603

Shen, Y. H., Godlewski, J., Zhu, J., Sathyanarayana, P., Leaner, V., Birrer, M. J., … Tzivion, G. (2003). Cross-talk between JNK/SAPK and ERK/MAPK pathways: Sustained activation of JNK blocks ERK activation by mitogenic factors. *Journal of Biological Chemistry*, *278*(29), 26715–26721. https://doi.org/10.1074/jbc.M303264200

Shirangi, T. R., Zaika, A., & Moll, U. M. (2002). Nuclear degradation of p53 occurs during down-regulation of the p53 response after DNA damage. *The FASEB Journal : Official Publication of the Federation of American Societies for Experimental Biology*, *16*(3), 420–422. https://doi.org/10.1096/fj.01-0617fje

Sillibourne, J. E., & Bornens, M. (2010). Polo-like kinase 4: The odd one out of the family. *Cell Division*. https://doi.org/10.1186/1747-1028-5-25

Singh, S., Upadhyay, A. K., Ajay, A. K., & Bhat, M. K. (2007). p53 regulates ERK activation in carboplatin induced apoptosis in cervical carcinoma: A novel target of p53 in apoptosis. *FEBS Letters*, *581*(2), 289–295. https://doi.org/10.1016/j.febslet.2006.12.035

Smith, G., Carey, F. A., Beattie, J., Wilkie, M. J. V., Lightfoot, T. J., Coxhead, J., … Wolf, C. R. (2002). Mutations in APC, Kirsten-ras, and p53--alternative genetic pathways to colorectal cancer. *Proceedings of the National Academy of Sciences*, *99*(14), 9433–9438.

https://doi.org/10.1073/pnas.122612899

Soliman, A. S., Bondy, M. L., Raouf, A. A., Makram, M. A., Johnston, D. A., & Levin, B. (1999). Cancer mortality in Menofeia, Egypt: Comparison with US mortality rates. *Cancer Causes and Control*, *10*(5), 349–354. https://doi.org/10.1023/A:1008968701313

Sullivan, K. D., Galbraith, M. D., Andrysik, Z., & Espinosa, J. M. (2018). Mechanisms of transcriptional regulation by p53. *Cell Death and Differentiation*, *25*. https://doi.org/10.1038/cdd.2017.174

Swallow, C. J., Ko, M. A., Siddiqui, N. U., Hudson, J. W., & Dennis, J. W. (2005). Sak/Plk4 and mitotic fidelity. *Oncogene*. https://doi.org/10.1038/sj.onc.1208275

Tang, Z., Dai, S., He, Y., Doty, R. A., Shultz, L. D., Sampson, S. B., & Dai, C. (2015). MEK guards proteome stability and inhibits tumor-suppressive amyloidogenesis via HSF1. *Cell*, *160*(4), 729–744. https://doi.org/10.1016/j.cell.2015.01.028

Tovar, C., Rosinski, J., Filipovic, Z., Higgins, B., Kolinsky, K., Hilton, H., … Vassilev, L. T. (2006). Small-molecule MDM2 antagonists reveal aberrant p53 signaling in cancer: implications for therapy. *Proceedings of the National Academy of Sciences of the United States of America*, *103*, 1888–1893. https://doi.org/10.1073/pnas.0507493103

Trino, S., Iacobucci, I., Erriquez, D., Laurenzana, I., De Luca, L., Ferrari, A., … Martinelli, G. (2016). Targeting the p53-MDM2 interaction by the small-molecule MDM2 antagonist Nutlin-3a: a new challenged target therapy in adult Philadelphia positive acute lymphoblastic leukemia patients. *Oncotarget*, *7*(11), 12951–12961. https://doi.org/10.18632/oncotarget.7339

Unger, T., Nau, M., Segal, S., & Minna, J. (1992). p53: a transdominant regulator of transcription whose function is ablated by mutations occurring in human cancer. *EMBO Journal*, *11*(4), 1383–1390.

Vassilev, L. T., Vu, B. T., Graves, B., Carvajal, D., Podlaski, F., Filipovic, Z., … Liu, E. A. (2004). In Vivo Activation of the p53 Pathway by Small-Molecule Antagonists of MDM2. *Science*, *303*(5659), 844–848. https://doi.org/10.1126/science.1092472

Vogelstein, B., Lane, D., & Levine, A. J. (2000). Surfing the p53 network. *Nature*, *408*(6810), 307–310. https://doi.org/10.1038/35042675

Vousden, K. H., & Lane, D. P. (2007). p53 in health and disease. *Nature Reviews Molecular Cell Biology*. https://doi.org/10.1038/nrm2147

Vousden, K. H., & Lu, X. (2002). Live or let die: The cell's response to p53. *Nature Reviews Cancer*. https://doi.org/10.1038/nrc864

Vousden, K. H., & Prives, C. (2009). Blinded by the Light: The Growing Complexity of p53. *Cell*. https://doi.org/10.1016/j.cell.2009.04.037

Vousden, K. H., & Ryan, K. M. (2009). P53 and metabolism. *Nature Reviews Cancer*. https://doi.org/10.1038/nrc2715

Whitesell, L., & Lindquist, S. L. (2005). HSP90 and the chaperoning of cancer. *Nature Reviews Cancer*. https://doi.org/10.1038/nrc1716

Wu, C. (1995). Heat Shock Transcription Factors: Structure and Regulation. *Annual Review of Cell and Developmental Biology*, *11*(1), 441–469. https://doi.org/10.1146/annurev.cb.11.110195.002301

Zhang, H., Wu, W., Du, Y., Santos, S. J., Conrad, S. E., Watson, J. T., … Gallo, K. A. (2004). Hsp90/p50cdc37Is Required for Mixed-lineage Kinase (MLK) 3 Signaling. *Journal of Biological Chemistry*, *279*(19), 19457–19463. https://doi.org/10.1074/jbc.M311377200

Zhang, P., Kawakami, H., Liu, W., Zeng, X., K, S., Tao, K., … Sinicrope, F. (2018). Targeting CDK1 and MEK/ERK Overcomes Apoptotic Resistance in BRAF-Mutant Human Colorectal Cancer.

Zhang, W., Liu, H. T., & Tu LIU, H. (2002). MAPK signal pathways in the regulation of cell proliferation in mammalian cells. *Cell Research*, *12*(1), 9–18. https://doi.org/10.1038/sj.cr.7290105

7. STATUTORY DECLARATION

I hereby assure that I have composed the present thesis entitled *"Wild-type p53 suppresses the tumor-driving HSF1 activity in colorectal cancer"* independently and have used no other appliances than indicated. Parts being gathered from other works according to wording or meaning I have indicated in every single case by declaration of source.

I hereby state furthermore, that I have produced my works according to the principles of good scientific practise in compliance with the valid "Richtlinen der Georg-August-Universität Göttingen zur Sicherung guter wissenschaftlicher Praxis".

Date: 28.05.2018

Name: Özge Çiçek Şener

Signature: